國 立 交 通 大 學

物理研究所

碩 士 論 文

強雷射脈衝導致非線性原子激發之 Fourier-Floquet 分析

Fourier-Floquet analysis of highly nonlinear atomic excitation by intense femto-second laser pulses

研究生 ： 韓宗潔

指導教授 ： 寺西慶哲 教授

中華民國一百零三年七月

強雷射脈衝導致非線性原子激發之 Fourier-Floquet 分析

Fourier-Floquet analysis of highly nonlinear atomic excitation by intense femto-second laser pulses

研究生 ： 韓宗潔　　Student : Zung-Jie Han

指導教授 ： 寺西慶哲 教授　　Advisor : Yoshiaki Teranishi

國 立 交 通 大 學
物 理 研 究 所
碩 士 論 文

A Thesis
Submitted to Institute of Physics
College of Science
National Chiao-Tung University
in Partial Fulfillment of the Requirements
for the Degree of
master in

Physics

July 2014

Hsinchu, Taiwan, Republic of China

中華民國一百零三年七月

強雷射脈衝導致非線性原子激發之 Fourier-Floquet 分析

學生 ： 韓宗潔　　指導教授 ： 寺西慶哲 教授

國立交通大學物理研究所碩士班

摘要

近年來由強飛秒雷射所產生的現象已受到理論上和實驗上的關注。當一個分子受到強飛秒雷射的激發時，所發射出來的螢光訊號已被證實是來自於中性的分子碎片，此被稱為"中性分裂"的現象被視為可以發展雷射應用的重要關鍵。造成此現象的機制或許可被解釋成以下：經由雷射的非線性激發，分子先處於高激發態，然後再經由解離變成許多電子激發態的中性分子碎片，最後散發出螢光訊號。儘管我們了解此現象的重要性，但是對於其中的高非線性激發的理論機制還未被完整的了解。

在此論文中，我們選取氫原子作為模擬系統並應用 Fourier-Floquet 光譜去檢視高非線性激發的理論機制，經由以上方法我們成功了提出相同奇偶的角動量最終激發態擁有相同的激發機制。另外，一般被視為只能適用於弱微擾場下的"Ramsey fringe"也被我們證實了在高非線性激發過程也是適用的。

Fourier-Floquet analysis of highly nonlinear atomic excitation by intense femto-second laser pulses

Student : Zung-Jie Han Advisor : Dr. Yoshiaki Teranishi

Institute of Physics
National Chiao Tung University

Abstract

The atomic and molecular processes induced by intense (~10^{14} W/cm^2) femto-second (10^{-15} s) lasers have attracted significant attention, both theoretical and experimental. When an intense femto-second laser is irradiated to a molecule, fluorescence signals are emitted from neutral fragments of the molecule. This phenomenon, called the neutral fragmentation, is expected to open new possibilities in laser technologies such as remote sensing and remote lasing. The mechanism may be understood as: (1) highly nonlinear excitation of the molecule, (2) the dissociation of the excited state molecule into electronically excited neutral fragments, (3) fluorescence from the neutral fragments. In spite of its importance, the mechanism of the highly nonlinear excitation has not been well understood.

In this thesis, we take hydrogen atom as an example to examine the mechanism of the highly nonlinear excitation using the Fourier-Floquet spectra. We succeeded in proposing the detailed mechanism, which we find different depending on the parity of the angular momentum of the final state. Furthermore we have shown that the Ramsey fringe, which is believed only applicable in the perturbatively weak field, works nicely in highly nonlinear processes.

Acknowledgement

I would like to thank all the people who help me in these years. Without their help, I could not finish this research by myself. They have not only taught me, inspire me but also reached out their hands when I was low. A thousand thanks may not be enough to describe my grateful heart.

First, my deepest gratitude goes first and foremost to Prof. Teranishi, my supervisor, for his constant encouragement and guidance. He has walked me through all the stages of the writing of this thesis. Without his consistent and illuminating instruction, this thesis could not have reached its present form. Second, I would like to thank all the member in our group not only for their help when I was stuck with unsolved problem, but also for sparing time to listen to me. Last but not least, my thanks would go to my beloved family and my girlfriend for their loving considerations and great confidence in me all through these years; especially my girlfriend, who had devoted her time and patience when I needed them the most.

A million thanks to these people, for what they had done for me has shown in this thesis. It represents not only my own study in these years but also represents their dedication to me. Finally, I hope this thesis study has done themselves proud.

Contents

List of Figures

This Floquet spectrum is associated with the initial state is 7th excited state(4p).

Figure 3-4(h) Fourier transform the excitation probability amplitude into frequency domain. This Floquet spectrum is associated with the initial state is 8th excited state(4d).

Figure 3-4(i) Fourier transform the excitation probability amplitude into frequency domain. This Floquet spectrum is associated with the initial state is 9th excited state(4f).

Figure 3-4(j) Fourier transform the excitation probability amplitude into frequency domain. This Floquet spectrum is associated with the initial state is 10th excited state(5s).

Figure 3-4(k) Fourier transform the excitation probability amplitude into frequency domain. This Floquet spectrum is associated with the initial state is 11th excited state(5p).

Figure 3-4(l) Fourier transform the excitation probability amplitude into frequency domain. This Floquet spectrum is associated with the initial state is 12th excited state(5d).

Figure 3-4(m) Fourier transform the excitation probability amplitude into frequency domain. This Floquet spectrum is associated with the initial state is 13th excited state(5f).

Figure 3-4(n) Fourier transform the excitation probability amplitude into frequency domain. This Floquet spectrum is associated with the initial state is 14th excited state(5g).

Figure 3-5 Fourier transforming the transition probability, which is induced by the double intense laser pulses, into frequency domain. Here, the pulse has intensity about 1.4×10^{14}W/cm^2. The laser pulse duration is about 10fs(FWHM), and the wavelength of the laser pulse is 800nm.

I. Introduction

Since laser was invented by Charles Townes and Arthur Schawlow in 1950s [1], it has been widely used in various fields both of science and technology. If a weak laser is irradiated, atoms/molecules do not change their original characters significantly, and the perturbation theory is applicable to describe the dynamics. When atoms/molecules interact with an intense laser, on the other hand, various types of complicated processes take place. Examples are above-threshold ionization [2], dressed-state formation [3], tunneling ionization [4], etc.

If the laser intensity is greater than 10^{12} W/cm^2, structure change in molecules becomes possible. When the intensity is around $10^{14} - 10^{15}$ W/cm^2, tunneling ionization takes place, in which electron(s) are emitted under the tunneling process through the potential barrier induced by the Coulomb potential and the laser fields. Once electrons are kicked out, some of the chemical bonds are broken, and a drastic dissociation may take places due to the repulsive Coulomb interactions between ionic fragments. In general, when an intense laser is applied to molecules, most of molecules are believed to dissociate into ionic fragments.

If the ejected electrons behave as plasma, a new phenomenon so-called "Filamentation" is induced. When an intense laser pulse is focused on a transparent material, the refractive index of the material is modified depending on the intensity of the laser due to the Kerr effect. The spatial dependence of the laser intensity gives rise to position dependent refractive index, which acts as a lens to focus the laser beam (self-focusing). When the laser beam is focused, the power of laser may be amplified enough to ionize the material and the plasma is created in the trail of laser. When the plasma becomes saturated, the refractive index of the material decreases. That causes beam defocusing, and it is called "self-defocusing". Filamentation occurs as a consequence of dynamic balance between self-focusing and defocusing effects in the electron plasma [5], to stabilize the peak intensity for a long distance. The filamentation

was discovered in 1995 [6], and many papers have been published to discuss the filamentation in different materials and its application. There are various applications of filamentation proposed so far, such as remote sensing [7], remote lasing [8], lighting control [9], etc.

The electronic excitation of molecule induced by an intense laser field has attracted significant attention since the discovery of "neutral fragmentation" [10]. In their first experiment, methane molecules are placed in a vacuum chamber and a Ti-sapphire laser with intensity around $10^{14} - 10^{15}$ W/cm^2 is applied to the target molecules. A spectrometer is placed next to the vacuum chamber to detect the photons coming from the chamber. The positions of the peaks in the spectrum of the photons shown in Fig. 1-1 coincide with the spectra of neutral CH, which implies that the observed photons are the fluorescence from neutral CH fragments, not from ionized fragments. They consider that the neutral CH fragments are produced by the excitation of the methane molecule into anti-bonding states. They also obtained the fluorescence signals versus the laser intensity as shown in Fig. 1-2. The result shows that the fluorescence signals have a power dependence on the laser intensity. The large value of the slope (n=10) may indicate that a high order perturbation plays an important role in this type of transition. Assuming that 10 photons are absorbed, the transition energy exceeds the ionization potential of methane (~12.6eV). This is why they claim that the fluorescence signals are attributed to such highly energized states known as the super-excited states. Similar phenomena of neutral dissociation can be seen in different target molecules, such as hydrogen molecules [11], oxygen molecule [12], nitric oxide molecules [13], etc. Here, we take oxygen molecule as an example to introduce the phenomena more in detail.

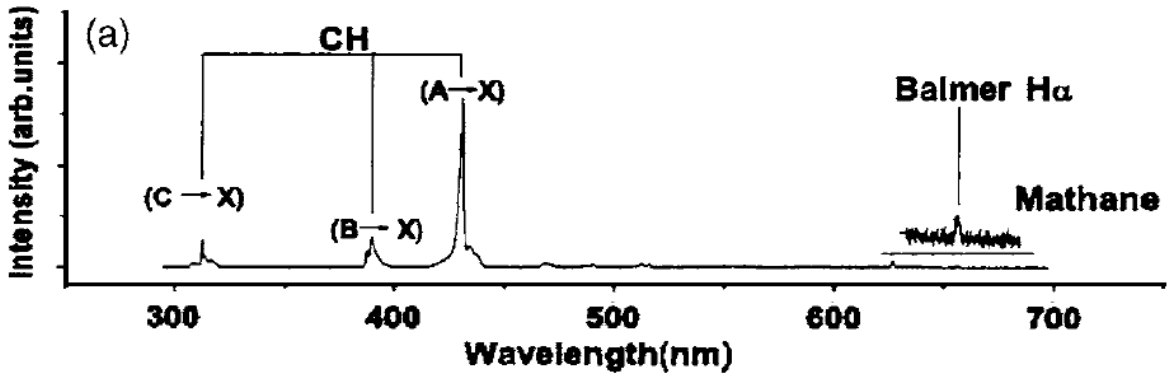

Figure1-1 The fluorescence spectra of methane CH_4 taken from Ref. [10].

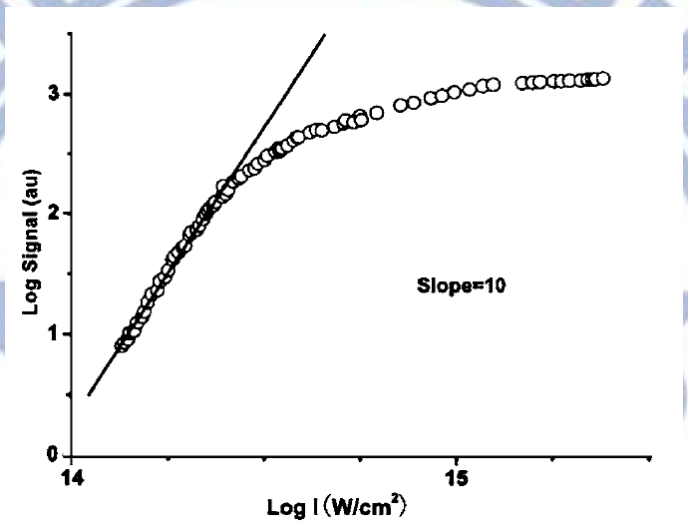

Figure1-2 The laser intensity dependence of the CH (*A*→*X*) fluorescence intensity. The rising slope of the curve is 10±1, taken from Ref. [10].

The experiment with oxygen molecule as a target molecule was done by Song *et al*. in 2010 [12]. The spectrum of the fluorescence shown in Fig. 1-3 implies that they are all coming from neutral fragments of oxygen atom, not ionized. The fluorescence signals versus the laser intensity in Fig. 1-4 shows similar tendencies as those of methane: (1) The fluorescence signals have a power dependence on laser intensity, and (2) The absorbing energy of photons are larger than the ionization potential of the target molecule.

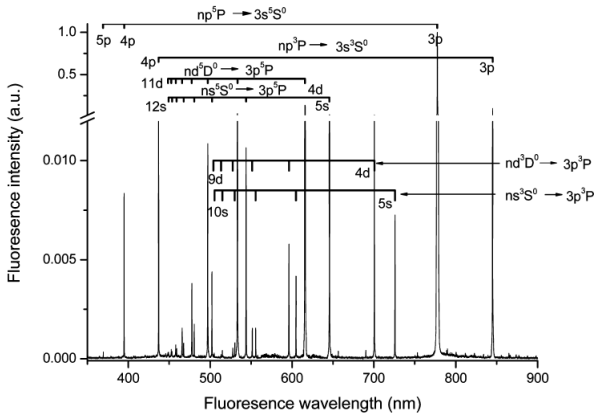

Figure1-3 The fluorescence spectrum of the photodissociation products. The target molecule is oxygen, taken from Ref. [12]

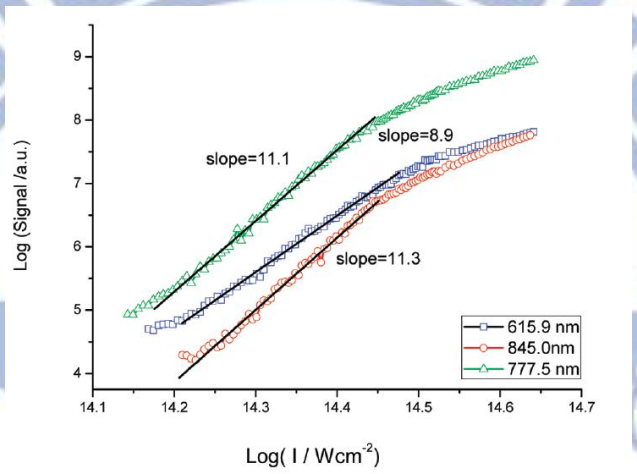

Figure1-4 Flourescence intensity dependence on the laser intensity. The fluorescence is collected and integrated around 615.9, 77.5 and 845.0nm in Fig.1-3, respectively. This experiment are also done by D. Song *et al*. in 2010.taken from Ref. [12]

In order to explain these experiments, Teranishi *et al* proposed the three-step mechanism [14], which consists of excitation, dissociation and fluorescence (see Fig. 1-5). When the target molecule is irradiated by an intense laser pulse, electronic excitation takes place in the molecule. Then (mainly after the laser pulse is turned off), the molecule dissociates into neutral fragments. After that, the spontaneous emission from the excited fragments occurs. The theoretical calculation including all of the three steps is difficult, and it is thus hard to calculate the fluorescence intensities to reproduce the experimental results. However, the excitation probabilities of molecules before the dissociation can be calculated easily, if we ignore the nuclear motion and the electronic continuum (superexcited states are also ignored).

Under these assumptions, they calculated the excitation probabilities for oxygen molecular target (see Fig. 1-6), and they show a similar tendency as that of fluorescence intensity in Fig. 1-4. They concluded that the fragmentation occurs through excited states of molecule, not through superexcited states. It is difficult, however, to confirm this conclusion in experiment, because they can observe only the fluorescence signals from the fragments, which do not provide the information of intermediate states.

In this thesis, we perform numerical simulations of highly nonlinear excitation of hydrogen atom by femto second intense laser fields to reveal the detailed dynamics. First, we calculate the excitation probability of hydrogen atom as function of laser intensity. Second, we calculate the transition probability amplitudes as functions of time. We use the Fourier-Floquet analysis to understand the dynamics during the transition in intense laser fields. Third, based on the Fourier-Floquet analysis we show that so called the Ramsey fringe is observed in intense field region as well, and propose a new experimental scheme to provide the information on the intermediate states.

The rest of the thesis is organized as follows. In the next chapter we summarize basic theories for the quantum dynamics induced by a time dependent interaction. In chapter III, the results of our numerical calculation is presented. The summary of this thesis is given in chapter IV.

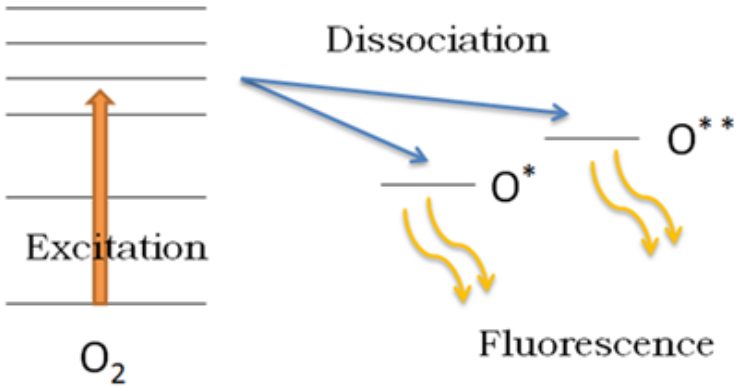

Figure1-5 The three-step mechanism was proposed to explain the observed fluorescence signals by Prof. Teranishi in 2010, which are excitation, dissociation and fluorescence.[12]

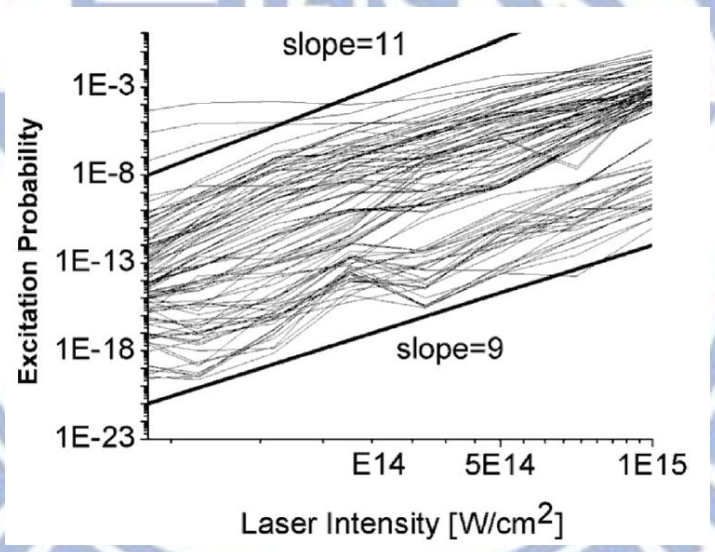

Figure1-6 Excitation probabilities to various excited states of O_2 as functions of laser intensity. Here, the laser pulse duration time is 42fs, and the central frequencies of the laser pulse are 800nm. This theoretical calculation is done by Prof. Teranishi in 2010.[12]

II. The Theory

2.1 Review

In most cases, quantum mechanical time dependent problems cannot be solved directly. We usually need approximations to simplify the problems so that we can obtain the analytical solutions. In this research, we focus on the problem of atom-laser interaction. In this chapter, we summarize the basic theories related to our research such as the perturbation approximation, rotating wave approximation and Floquet theory. Here we start by the basic formulation of the time dependent problems in quantum mechanics.

Time-dependent quantum mechanical problem:

Here we consider the time-dependent quantum mechanics with the time-dependent Hamiltonian given by

$$\hat{H}(t) = \hat{H}_0 + \hat{H}'(t), \tag{1}$$

where $\hat{H}_0$ is the unperturbed Hamiltonian, and $\hat{H}'(t)$ is the time-dependent part of the Hamiltonian, which describes the atom-laser interaction in this thesis. The time dependent wave function $|\Psi(t)\rangle$ can be obtained as the solution of the time-dependent Schrodinger equation:

$$i\hbar\partial_t|\Psi(t)\rangle = \hat{H}(t)|\Psi(t)\rangle. \tag{2}$$

The wave function can be expressed as a linear combination of the eigen states of the unperturbed Hamiltonian $\hat{H}_0$ with the time-dependent coefficient $c_n(t)$, namely

$$|\Psi(t)\rangle = \sum_n c_n(t)\,|\varphi_n\rangle, \tag{3}$$

where $|\varphi_n\rangle$ is the eigenstate of $\hat{H}_0$, which has the properties of orthonormality and completeness:

$$\langle\varphi_n|\varphi_m\rangle = \delta_{nm}, \qquad \text{(Orthonormality)} \tag{4}$$

and

$$\sum_n |\varphi_n\rangle\langle\varphi_n| = I, \qquad \text{(completeness)} \tag{5}$$

Here δ_{nm} and I are the Kronecker delta and the identity operator, respectively.

Propagation:

The time evolution operator, usually denoted by $\hat{U}(t, t_0)$ transforms the wave function $|\Psi(t_0)\rangle$ at a time t_0 to $|\Psi(t)\rangle$ at a time t:

$$|\Psi(t)\rangle = \hat{U}(t, t_0)|\Psi(t_0)\rangle. \tag{6}$$

Substituting Eq. (6) into the Schrodinger equation Eq. (2), we obtain

$$i\hbar\partial_t \hat{U}(t, t_0)|\Psi(t_0)\rangle = \hat{H}\hat{U}(t, t_0)|\Psi(t_0)\rangle. \tag{7}$$

This equation should hold for arbitrary initial wave function $|\Psi(t_0)\rangle$, thus we have

$$i\hbar\partial_t \hat{U}(t, t_0) = \hat{H}\hat{U}(t, t_0). \tag{8}$$

This is the differential equation for the time evolution operator, which should be solved with the boundary condition $\hat{U}(t_0, t_0) = I$. Integrating both side of Eq.(8) with taking the boundary condition into account, we obtain the integral equation for the time evolution operator,

$$U_{\mathrm{I}}(t, t_0) = \mathrm{I} - \frac{i}{\hbar}\int_{t_0}^{t} d\tau_1 V_{\mathrm{I}}(\tau_1) U_{\mathrm{I}}(\tau_1, t_0). \tag{9}$$

Time evolution operator has the following properties:

1. The time evolution operator is identity, when $t = t_0$:

$$\lim_{t \to t_0} \hat{U}(t, t_0) = 1. \tag{10}$$

2. The propagator should preserve the normalization of wave functions. That is, if a wave function $|\Psi\rangle$ is normalized at t_0, it should also be normalized at later times t

$$\langle\Psi(t_0)|\Psi(t_0)\rangle = \langle\Psi(t)|\Psi(t)\rangle, \tag{11}$$

$$= \langle\Psi(t_0)|\hat{U}^{\dagger}(t, t_0)\hat{U}(t, t_0)|\Psi(t_0)\rangle, \tag{12}$$

which implies $\hat{U}^{\dagger}(t, t_0)\hat{U}(t, t_0) = 1$ or $\hat{U}^{\dagger}(t, t_0) = \hat{U}^{-1}(t, t_0)$. Therefore the propagator $\hat{U}(t, t_0)$ is a unitary operator

3. The propagator $\hat{U}(t, t_0)$ should satisfy the composition property

$$\hat{U}(t,t_0) = \hat{U}(t,t_1)\hat{U}(t_1,t_0), \tag{13}$$

which means that the propagation from t_0 to t can be decomposed into the propagations from t_0 to t_1 and from t_1 to t.

Representation:

Here, we introduce three representations of the state vector: the Schrodinger representation, the Heisenberg representation, and the interaction representation.

Assume we have a wave function $|\Psi(t)\rangle$ and an observable operator $\hat{O}$. The expectation value of the observable is given by

$$\langle O\rangle = \langle\Psi(t)|\hat{O}|\Psi(t)\rangle. \tag{14}$$

The wave function in Eq. (14) can be represented using the time evolution operator and the initial wave function $|\Psi(t_0)\rangle$:

$$\langle O\rangle = \langle\Psi(t_0)|U^{-1}(t,t_0)\hat{O}U(t,t_0)|\Psi(t_0)\rangle. \tag{15}$$

In the Schrodinger representation, the state vector evolves in time:

$$|\Psi\rangle_s = |\Psi(t)\rangle, \tag{16}$$

but observables does not:

$$\hat{O}_S = \hat{O}. \tag{17}$$

Equation (15), may be understood as follows. The state vector is defined as

$$|\Psi\rangle_H = |\Psi(t_0)\rangle, \tag{18}$$

which does not depend on time, whereas the observables defined by

$$\hat{O}_H = U^{-1}(t,t_0)\hat{O}U(t,t_0) = \hat{O}(t), \tag{19}$$

depends on time. This is called the Heisenberg representation. From Eqs. (16) and (18), we obtain the relation between state vectors in the Schrodinger representation and in the Heisenberg representation as

$$|\Psi\rangle_H = U^{-1}(t,t_0)|\Psi\rangle_S. \tag{20}$$

Now we introduce the interaction representation, which is an intermediate representation

between the Schrodinger representation and the Heisenberg representation, since both the state vector and the observables evolve in time. We define the state vector in the interaction representation with a unitary transformation:

$$|\Psi(t)\rangle_I = U_I^{-1}(t,t_0)|\Psi(t)\rangle_S, \tag{21}$$

where $U_I(t,t_0)$ is defined by $U_I(t,t_0) = e^{-i\hat{H}_0 t/\hbar}$.

The observables are transformed similarly to those in the Heisenberg representation in Eq.(19), namely

$$\hat{O}_I = U_I^{-1}(t,t_0)\hat{O}U_I(t,t_0) = e^{i\hat{H}_0 t/\hbar}\hat{O}e^{-i\hat{H}_0 t/\hbar}. \tag{22}$$

Atom-laser interaction:

Here, we introduce the atom-laser interaction under the semiclassical approximation, in which the laser field is treated classically, while the atom is treated quantum mechanically. The classical Hamiltonian of an electron in an electromagnetic field can be described with the scalar potential $\phi(\vec{r},t)$ and the vector potential $A(\vec{r},t)$:

$$\hat{H}(t) = \frac{1}{2m}\left(\hat{p} + \frac{e}{c}\vec{A}\right)^2 - e\phi \tag{23}$$

$$= \frac{\hat{p}^2}{2m} + \frac{e}{2mc}\left(\vec{A}\cdot\hat{p} + \hat{p}\cdot\vec{A}\right) + \frac{e^2}{2mc^2}\vec{A}^2 - e\phi, \tag{24}$$

where $\vec{p}$ is the momentum operator of an electron. In the Schrodinger picture, the momentum operator $\vec{p}$ is of the form:

$$\hat{p} = -i\hbar\vec{\nabla}. \tag{25}$$

Substituting the Hamiltonain in Eq. (24) into the Schrodinger equation, we have

$$i\hbar\partial_t|\Psi\rangle = \left[-\frac{\hbar^2}{2m}\vec{\nabla}^2 - i\hbar\frac{e}{2mc}\left(\vec{A}\cdot\vec{\nabla} + \vec{\nabla}\cdot\vec{A}\right) + \frac{e^2}{2mc^2}\vec{A}^2 - e\phi\right]|\Psi\rangle. \tag{26}$$

The term of $\vec{\nabla}\cdot\left(\vec{A}\Psi\right)$ in Eq. (26) can be expanded in the form:

$$\vec{\nabla}\cdot\left(\vec{A}\Psi\right) = \vec{A}\cdot\left(\vec{\nabla}\Psi\right) + \left(\vec{\nabla}\cdot\vec{A}\right)\Psi. \tag{27}$$

Since in the Coulomb gauge we have

$$\vec{\nabla}\cdot\vec{A} = 0, \tag{28}$$

the term $\vec{\nabla}\cdot\left(\vec{A}\Psi\right)$ in Eq. (27) becomes

$$\vec{\nabla}\cdot\left(\vec{A}\Psi\right)=\vec{A}\cdot\left(\vec{\nabla}\Psi\right). \tag{29}$$

Substituting Eq. (29) into the Schrodinger equation Eq. (26), we obtain

$$i\hbar\partial_t|\Psi\rangle=\left[-\frac{\hbar^2}{2m}\vec{\nabla}^2-i\hbar\frac{e}{mc}\vec{A}\cdot\vec{\nabla}+\frac{e^2}{2mc^2}\vec{A}^2-e\phi\right], \tag{30}$$

Here, we consider a hydrogenic atom in the electromagnetic field, so we add the Coulomb potential to the Hamiltonian given by

$$V(r)=-\frac{Ze}{(4\pi\epsilon_0)r}, \tag{31}$$

where Z is the nuclear charge, and r is the distance between the nucleus and the electron.

Then, the Schrodinger equation is

$$i\hbar\partial_t|\Psi\rangle=\left[-\frac{\hbar^2}{2m}\vec{\nabla}^2-i\hbar\frac{e}{mc}\vec{A}\cdot\vec{\nabla}+\frac{e^2}{2mc^2}\vec{A}^2-\frac{Ze}{(4\pi\epsilon_0)r}\right]. \tag{32}$$

This equation can be written as:

$$i\hbar\partial_t|\Psi\rangle=\left[\hat{H}_0+\hat{H}'(t)\right]|\Psi\rangle, \tag{33}$$

with

$$\hat{H}_0=-\frac{\hbar^2}{2m}\vec{\nabla}^2-\frac{Ze^2}{(4\pi\epsilon_0)r} \quad \text{and} \quad \hat{H}'(t)=-i\hbar\frac{e}{mc}\vec{A}\cdot\vec{\nabla}+\frac{e^2}{2mc^2}\vec{A}^2-e\phi.$$

The unperturbed Hamiltonian $\hat{H}_0$ describes the hydrogenic atom in vacuum, and the perturbation $\hat{H}'(t)$ describes the interaction between the atom and the laser field. According to the Maxwell's equation, the vector potential $A(\vec{r},t)$ satisfies

$$\vec{\nabla}^2\vec{A}-\frac{1}{c^2}\frac{\partial^2}{\partial t^2}\vec{A}=0. \tag{34}$$

The plane wave solution of Eq.(34) with the angular frequency ω is given by

$$A(\vec{r},t)=\hat{\epsilon}A_0\cos\left(\vec{k}\cdot\vec{r}-\omega t+\delta\right), \tag{35}$$

where $\vec{k}$ is the propagation vector of laser field, $\hat{\epsilon}$ is the polarization direction, and δ is a real constant phase. When the wavelength $(\lambda=\frac{2\pi}{|\vec{k}|})$ is sufficiently larger than the size of the atom, namely

$$\lambda\gg d_{atom}, \tag{36}$$

we can neglect the spatial variation of the vector potential (the dipole approximation),

$$A(\vec{r},t) \approx \vec{A}(t) = \hat{\epsilon}A_0 \cos(\omega t + \delta). \quad (37)$$

In the case of a pulsed laser, the vector potential is given by

$$A(t) = \hat{\epsilon}A_0(t) \cos(\omega t + \delta). \quad (38)$$

Here $A_0(t)$ is the envelope function. Finally we have the expression of the perturbation $\hat{H}'(t)$ given by

$$\hat{H}'(t) = -i\hbar\frac{e}{mc}\vec{A}(t)\cdot\vec{\nabla} + \frac{e^2}{2mc^2}\vec{A}(t)^2. \quad (39)$$

Here we consider the gauge transformations:

$$A \to A' = A + \nabla f, \quad (39)$$

$$\phi \to \phi' = \phi - \frac{1}{c}\frac{\partial f}{\partial t}, \quad (40)$$

$$\Psi \to \Psi' = \exp\left(-\frac{ief}{c\hbar}\right)\Psi, \quad (41)$$

where f is an arbitrary real function of $\vec{r}$ and t. We simplify the perturbation Eq. (39) by the gauge transformation. We use a function given by

$$f = -\vec{A}(t)\cdot\vec{r}. \quad (42)$$

Then, the gauge transformation reads

$$A' = 0, \quad (43)$$

$$\phi' = \frac{1}{c}\frac{\partial\vec{A}(t)}{\partial t}\cdot\vec{r} = -E(t)\cdot\vec{r}, \quad (44)$$

$$\Psi' = \exp\left(\frac{ie\vec{A}(t)}{c\hbar}\cdot\vec{r}\right)\Psi, \quad (45)$$

where $\vec{r}$ are the polarization of the electric field. Equation (44) implies that $\frac{1}{c}\frac{\partial\vec{A}(t)}{\partial t}$ equals the electric field of the laser $E(t)$. After the gauge transformation, the perturbation becomes:

$$\hat{H}'(t) = -E(t)\cdot\vec{r}. \quad (46)$$

Then, the Schrodinger equation is given by

$$i\hbar\partial_t|\Psi'\rangle = \left[\hat{H}_0 + eE(t)\cdot\vec{r}\right]|\Psi'\rangle. \quad (47)$$

2.2 Perturbation Theory

We consider a time-dependent Hamiltonian, given by

$$\hat{H}(t) = \hat{H}_0 + \hat{V}'(t), \tag{48}$$

where $\hat{H}_0$ is a time-independent Hamiltonian, which eigenvalue problem has been solved, and $\hat{V}'(t)$ is a time-dependent perturbation. The time-dependent Schrodinger may be hard to solve. The perturbation theory provides an approximated solution for small perturbation cases. The time-dependent Schrodinger equation in the interaction representation is given by

$$i\hbar\partial_t|\Psi(t)\rangle_{\mathrm{I}} = V_{\mathrm{I}}|\Psi(t)\rangle_{\mathrm{I}}, \tag{49}$$

where $V_{\mathrm{I}} = e^{i\hat{H}_0 t/\hbar}\, V' e^{-i\hat{H}_0 t/\hbar}$. The wave function $|\Psi(t)\rangle_{\mathrm{I}}$ can be represented with an initial wave function $|\Psi(t_0)\rangle_{\mathrm{I}}$ and the time-evolution operator, $U_{\mathrm{I}}(t, t_0)$, namely

$$|\Psi(t)\rangle_{\mathrm{I}} = U_{\mathrm{I}}(t, t_0)\, |\Psi(t_0)\rangle_{\mathrm{I}}. \tag{50}$$

Substituting the wave function Eq. (50) into the time dependent Schrodinger equation Eq. (49), we have

$$i\partial_t U_{\mathrm{I}}(t, t_0)\, |\Psi(t_0)\rangle_{\mathrm{I}} = V_{\mathrm{I}} U_{\mathrm{I}}(t, t_0)\, |\Psi(t_0)\rangle_{\mathrm{I}}, \tag{51}$$

or

$$[i\hbar\partial_t U_{\mathrm{I}}(t, t_0) - V_{\mathrm{I}} U_{\mathrm{I}}(t, t_0)]\, |\Psi(t_0)\rangle_{\mathrm{I}} = 0. \tag{52}$$

Since Eq. (52) holds for arbitrary initial wave function $|\Psi(t_0)\rangle_{\mathrm{I}}$, we have

$$i\hbar\partial_t U_{\mathrm{I}}(t, t_0) = V_{\mathrm{I}} U_{\mathrm{I}}(t, t_0). \tag{53}$$

This is the differential equation for the time evolution operator in the interaction representation. Integrating both side of Eq. (53) with the boundary condition $U_{\mathrm{I}}(t_0, t_0) = \mathrm{I}$, we obtain the integral equation:

$$U_{\mathrm{I}}(t, t_0) = \mathrm{I} - \frac{i}{\hbar}\int_{t_0}^{t} d\tau_1 V_{\mathrm{I}}(\tau_1) U_{\mathrm{I}}(\tau_1, t_0). \tag{54}$$

Equation (54) is an integral equation, which we solve using the perturbation theory as follows. Assuming the perturbation is weak, $V_{\mathrm{I}}(\tau_1) \approx 0$,we obtain the zeroth order solution

$$U_{\mathrm{I}}^{(0)} = \mathrm{I}. \tag{55}$$

Substituting the zeroth order solution into the right hand side of Eq. (54), we obtain the first order solution:

$$U_{\mathrm{I}}^{(1)} = \mathrm{I} - \frac{i}{\hbar}\int_{t_0}^{t} d\tau_1 V_{\mathrm{I}}(\tau_1). \tag{56}$$

We substitute the first order approximation into the right hand side of Eq. (54) to obtain the second order approximation given by

$$U_{\mathrm{I}}^{(2)} = \mathrm{I} - \frac{i}{\hbar}\int_{t_0}^{t} d\tau_1 V_{\mathrm{I}}(\tau_1) + (\frac{i}{\hbar})^2 \int_{t_0}^{t} d\tau_1 V_{\mathrm{I}}(\tau_1) \int_{t_0}^{\tau_1} V_{\mathrm{I}}(\tau_2) d\tau_2 \,. \tag{57}$$

Repeating the procedure of substituting the *n*th-order approximation into the right hand side of Eq. (54), we obtain the equation for the (*n*+1)th-order.

$$U_{\mathrm{I}}{}^{(n)}(t, t_0) = \sum_{k=0}^{n} \left(-\frac{i}{\hbar}\right)^k \int_{t_0}^{t} \mathrm{d}\tau_1 .. \int_{\mathrm{t0}}^{\tau_{k-1}} d\tau_k V_{\mathrm{I}}(\tau_1) V_{\mathrm{I}}(\tau_2) \ldots V_{\mathrm{I}}(\tau_k). \tag{58}$$

For the small perturbation $V_I(t)$, the third term of 2nd-order approximation in Eq. (57) can be neglected and it approximately equals to the 1st-order approximation

$$U_{\mathrm{I}}^{(2)} \approx \mathrm{I} - \frac{i}{\hbar}\int_{t_0}^{t} d\tau_1 V_{\mathrm{I}}(\tau_1) = U_{\mathrm{I}}^{(1)}, \tag{59}$$

which implies the convergence of the 1st-order approximation for small perturbation.

Here we represent the wave function as a linear combination of the eigen states of $\widehat{H}_0$:

$$|\Psi(t)\rangle_{\mathrm{I}} = \sum_n c_n(t)|\varphi_n\rangle. \tag{60}$$

Here we call $c_n(t)$ the probability amplitude on state *n*. We represent the wave function at time t with the time evolution operator and the initial wave function $|\Psi(t_0)\rangle_{\mathrm{I}}$, then Eq. (60) reads

$$U_{\mathrm{I}}(t, t_0)|\Psi(t_0)\rangle_{\mathrm{I}} = \sum_n c_n(t)|\varphi_n\rangle. \tag{61}$$

By inserting the identity operator into the left hand side of Eq. (61), we obtain the probability amplitude:

$$\sum_n |\varphi_n\rangle\langle\varphi_n|U_{\mathrm{I}}(t, t_0)|\Psi_i\rangle_{\mathrm{I}} = \sum_n c_n(t)|\varphi_n\rangle, \tag{62}$$

$$c_n\,(t) = \langle\varphi_n|U_{\mathrm{I}}(t, t_0)|\Psi_i\rangle_{\mathrm{I}}. \tag{63}$$

We can obtain the nth-order probability amplitude by substituting the nth-order time evolution operator into Eq. (63). Here, we assume the initial wave function is one of the eigen states,

$$|\Psi(t_0)\rangle_{\mathrm{I}} = |\varphi_m\rangle. \tag{64}$$

Then, the transition amplitude in various orders of perturbation are obtained as follows:

Zero-order:

$$c_n^{(0)}(t) = \langle\varphi_n|U_{\mathrm{I}}^{(0)}(t,t_0)|\varphi_m\rangle, \tag{65}$$

$$= \langle\varphi_n|\mathrm{I}|\varphi_m\rangle = \delta_{nm}, \tag{66}$$

$$c_n^{(0)}(t) = \delta_{nm}. \tag{67}$$

First-order:

$$c_n^{(1)}(t) = \langle\varphi_n|U_{\mathrm{I}}^{(1)}(t,t_0)|\varphi_m\rangle, \tag{68}$$

$$= \delta_{nm} - \frac{i}{\hbar}\int_{t_0}^{t} d\tau\, e^{\frac{i\tau(E_n-E_m)}{\hbar}}\langle\varphi_n|V(\tau)|\varphi_m\rangle, \tag{69}$$

$$= \delta_{nm} - \frac{i}{\hbar}\int_{t_0}^{t} d\tau\, e^{i\omega_{nm}\tau}\, V_{nm}(\tau), \tag{70}$$

where $V_{nm}(t) = \langle\varphi_n|V(t)|\varphi_m\rangle$, and $\omega_{nm} = (E_n - E_m)/\hbar$, which we call the transition frequency.

Second-order:

$$c_n^{(2)}(t) = \langle\varphi_n|U_{\mathrm{I}}^{(2)}(t,t_0)|\varphi_m\rangle, \tag{71}$$

$$= \delta_{nm} - \frac{i}{\hbar}\int_{t_0}^{t} d\tau\, e^{i\omega_{nm}\tau}\, V_{nm}(\tau)$$

$$+\left(\frac{i}{\hbar}\right)^2 \sum_m \int_{t_0}^{t} d\tau_1 \int_{t_0}^{\tau_1} d\tau_2\, e^{i\omega_{nk}\tau_1 + i\omega_{km}\tau_2}\, V_{nk}(\tau_1)\, V_{km}(\tau_2) \tag{72}$$

The transition probability from the initial state $|\varphi_m\rangle$ to a final state $|\varphi_n\rangle$ at the final time t is given by

$$P_{m\to n} = |c_n(t)|^2. \tag{73}$$

Now we discuss some properties of the 1st-order perturbation theory. The 1st-order transition probability amplitude in Eq. (70) is a linear function with respect to the interaction potential $V_{nm}(\tau)$, which leads to the properties of additivity and homogeneity.

Suppose the potential is the sum of two potentials:

$$\hat{V}(t) = \hat{V}_a(t) + \hat{V}_b(t). \tag{74}$$

The first-order probability amplitudes of the respective potentials are:

$$c_n^{(1)}(t) = -\frac{i}{\hbar}\int_{t_0}^{t} d\tau\, e^{i\omega_{nm}d\tau}\langle\varphi_n|\hat{V}_a(\tau)|\varphi_m\rangle = \alpha\,, \tag{75}$$

and

$$c_n^{(1)}(t) = -\frac{i}{\hbar}\int_{t_0}^{t} d\tau\, e^{i\omega_{nm}d\tau}\langle\varphi_n|\hat{V}_b(\tau)|\varphi_m\rangle = \beta. \tag{76}$$

The first-order probability amplitude of the total potential in Eq. (74) is

$$c_n^{(1)}(t) = -\frac{i}{\hbar}\int_{t_0}^{t} d\tau\, e^{i\omega_{nm}d\tau}\, V_{nm}(\tau), \tag{77}$$

$$= -\frac{i}{\hbar}\int_{t_0}^{t} d\tau\, e^{i\omega_{nm}d\tau}\langle\varphi_n|\hat{V}_a(\tau)+\hat{V}_b(\tau)|\varphi_m\rangle, \tag{78}$$

$$= -\frac{i}{\hbar}\int_{t_0}^{t} d\tau\, e^{i\omega_{nm}d\tau}\langle\varphi_n|\hat{V}_a(\tau)|\varphi_m\rangle - \frac{i}{\hbar}\int_{t_0}^{t} d\tau\, e^{i\omega_{nm}d\tau}\langle\varphi_n|\hat{V}_b(\tau)|\varphi_m\rangle, \tag{79}$$

$$= \alpha + \beta\,. \tag{80}$$

The probability amplitude of the total potential is the sum of the two probability amplitudes given by Eq. (75) and Eq. (76), respectively. This property is called the additivity. Next, let us assume a potential given by

$$\hat{V}(t) = c\hat{V}_a(t), \tag{81}$$

where *c* is a complex constant. The 1st-order probability amplitude is given by

$$c_n^{(1)}(t) = -\frac{i}{\hbar}\int_{t_0}^{t} d\tau\, e^{i\omega_{nm}\tau}\langle\varphi_n|c\hat{V}_a(\tau)|\varphi_m\rangle, \tag{82}$$

$$= -\frac{ci}{\hbar}\int_{t_0}^{t} d\tau\, e^{i\omega_{nm}\tau}\, V_{nm}(\tau) = c\alpha. \tag{83}$$

The probability amplitude is *c* times the probability amplitude with the potential $\hat{V}_a(t)$. This is called the "homogeneity".

Hereafter, we discuss how to use the perturbation theory by taking two cases as examples: CW laser field and Gaussian pulse laser. Suppose the electric field of linearly polarized CW laser field with the driving frequency ω and the polarization direction z

$$\hat{E}(t) = E_0\sin(\omega t)\hat{k}, \tag{84}$$

where E_0 is the electric field amplitude. The interaction potential is given by

$$\hat{V}(t) = -qzE_0\sin(\omega t), \tag{85}$$

where q is the electron charge. Substituting this into the 1st-order probability amplitude in Eq. (68), we have

$$c_n^{(1)}(\infty) = -\frac{i}{\hbar}\int_{-\infty}^{\infty} dt\, e^{i\omega_{nm}t}\langle\varphi_n|-qzE_0\sin(\omega t)|\varphi_m\rangle. \tag{86}$$

We factor out $-qE_0\langle\varphi_n|z|\varphi_m\rangle$ in the above equation, then we obtain

$$c_n^{(1)}(\infty) = \frac{i}{\hbar}qE_0\langle\varphi_n|z|\varphi_m\rangle\int_{-\infty}^{\infty} dt\, e^{i\omega_{nm}t}\sin(\omega t). \tag{87}$$

The integral in Eq. (87) is the Fourier transform of the sinusoidal function with time. Thus we have

$$c_n^{(1)}(\omega) = \frac{i}{\hbar}qE_0\langle\varphi_n|z|\varphi_m\rangle\delta(\omega_{nm}-\omega). \tag{88}$$

The transition takes place only when the driving frequency ω is equal to the transition frequency ω_{nm}. This is called the resonance. Next let us consider a Gaussian pulse given by

$$\hat{E}(t) = E_0\sin(\omega t)e^{-t^2/\tau}\hat{k}, \tag{89}$$

where ω, $\hat{k}$, $\hat{\tau}$ are the driving frequency, the polarization vector, and the duration time, respectively.

The interaction potential is given by

$$\hat{V}(t) = -qzE_0\sin(\omega t)e^{-t^2/\tau}. \tag{90}$$

Substituting Eq. (90) into the 1st-order probability amplitude in Eq. (68), we obtain

$$c_n^{(1)}(\infty) = -\frac{i}{\hbar}\int_{-\infty}^{\infty} dt\, e^{i\omega_{nm}t}\langle\varphi_n|-qzE_0\sin(\omega t)e^{-t^2/\tau}|\varphi_m\rangle. \tag{91}$$

Factoring out $-qE_0\langle\varphi_n|z|\varphi_m\rangle$ in Eq. (91), we have

$$c_n^{(1)}(\infty) = \frac{i}{\hbar}qE_0\langle\varphi_n|z|\varphi_m\rangle\int_{-\infty}^{\infty} dt\, e^{i\omega_{nm}t}\langle\varphi_n|\sin(\omega t)e^{-t^2/\tau}|\varphi_m\rangle. \tag{92}$$

By replacing the sinusoidal function in Eq. (92) by $(e^{i\omega t}-e^{i\omega t})/2i$, we have

$$c_n^{(1)}(\infty) = \frac{1}{2\hbar}qE_0\langle\varphi_n|z|\varphi_m\rangle\int_{-\infty}^{\infty} dt[e^{i(\omega-\omega_{nm})t}-e^{i(\omega+\omega_{nm})t}]e^{-\frac{t^2}{\tau}}. \tag{93}$$

$$= \frac{1}{2\hbar} qE_0 \langle \varphi_n | z | \varphi_m \rangle \int_{-\infty}^{\infty} dt e^{i(\omega-\omega_{nm})t} e^{-\frac{t^2}{\tau}} - \int_{-\infty}^{\infty} e^{i(\omega+\omega_{nm})t} e^{-\frac{t^2}{\tau}}. \quad (94)$$

The integrals in Eq. (94) are the Fourier transforms of the Gaussian pulses, the transition amplitude is given by

$$c_n^{(1)}(\omega) = \frac{1}{2\hbar} qE_0 \langle \varphi_n | z | \varphi_m \rangle \left[\sqrt{\pi\tau} e^{-4\tau(\omega+\omega_{nm})^2} - \sqrt{\pi\tau} e^{-4\tau(\omega-\omega_{nm})^2} \right]. \quad (95)$$

The probability amplitude is proportional to the electric field amplitude and the square root of the pulse duration.

2.3 Rotating wave approximation

The rotating wave approximation is an approximation, which is valid when the perturbed Hamiltonain is a sinusoidal function and the driving frequency is close to the transition frequency (near resonance case). In the following, we introduce the rotating wave approximation. Suppose we have a two-level system with eigenvalue E_a , E_b and eigen states $|a\rangle, |b\rangle$, respectively, which is perturbed by a sinusoidal time-dependent potential with the driving frequency ω:

$$\hat{V}(\vec{r}, t) = v(\vec{r}) \sin(\omega t). \quad (96)$$

According to the first-order perturbation theory in Eq. (68), the transition probability amplitude is

$$c_b^{(1)}(t) = -\frac{i}{\hbar} \langle a | v(\vec{r}) | b \rangle \int_{t_0}^{t} d\tau \, e^{i\omega_{ab}\tau} \sin(\omega\tau), \quad (97)$$

where $\omega_{ab} = (E_a - E_a)/\hbar$. We replace $\sin(\omega t)$ by $(e^{i\omega t} - e^{-i\omega t})/2i$ in Eq. (97), and then take the integral to obtain

$$c_b^{(1)}(t) = \frac{V_{ab}}{2\hbar} \int_{t_0}^{t} \left[e^{i(\omega_{ab}+\omega)\tau} - e^{i(\omega_{ab}-\omega)\tau} \right] d\tau \quad (98)$$

$$= \frac{V_{ab}}{2\hbar} \left[\frac{e^{i(\omega_{ab}+\omega)t} - 1}{\omega_{ab} + \omega} - \frac{e^{i(\omega_{ab}-\omega)t} - 1}{\omega_{ab} - \omega} \right]. \quad (99)$$

In the near resonance case, i.e. $\omega_{ab} + \omega \gg |\omega_{ab} - \omega|$, the second term in the square brackets in Eq. (99) dominates, and the first term can be ignored. Then, the transition probability amplitude is approximated as:

$$c_b^{(1)}(t) \cong \frac{V_{ab}}{2\hbar}\left[\frac{e^{i(\omega_{ab}-\omega)t}-1}{\omega_{ab}-\omega}\right] \tag{100}$$

$$= \frac{V_{ab}e^{\frac{i(\omega_{ab}-\omega)}{2}}}{2\hbar(\omega_{ab}-\omega)}\left[e^{\frac{i(\omega_{ab}-\omega)}{2}} - e^{-\frac{i(\omega_{ab}-\omega)}{2}}\right] \tag{101}$$

$$= i\frac{V_{ab}}{\hbar}\frac{\sin[(\omega_{ab}-\omega)t/2]}{\omega_{ab}-\omega}e^{\frac{i(\omega_{ab}-\omega)}{2}}. \tag{102}$$

Then, the transition probability in near resonance condition is a simple analytic form with sinusoidal function:

$$P_{a\to b} = |\, c_b(t)|^2 \cong \frac{|V_{ab}|^2}{\hbar^2}\frac{\sin^2[(\omega_{ab}-\omega)t/2]}{(\omega_{ab}-\omega)^2}. \tag{103}$$

According to Eq. (100), instead of ignoring the first term in the square brackets in Eq. (99) we can approximate the potential as:

$$H'_{ab} = -\frac{V_{ab}}{2i}e^{i\omega t} \quad \text{and} \quad H'_{ba} = \frac{V_{ba}}{2i}e^{-i\omega t} \tag{104}$$

This approximation is so-called the rotating wave approximation. Using the rotating wave approximation, the time-dependent Schrodinger equation can be directly solved without using the perturbation theory as shown in the following.

The wave function Ψ can be expressed as a linear combination of the eigen states $|a\rangle, |b\rangle$

$$|\Psi(t)\rangle = c_a(t)e^{-\frac{iE_a t}{\hbar}}|a\rangle + c_b(t)e^{-\frac{iE_b t}{\hbar}}|b\rangle. \tag{105}$$

The time-dependent Schrodinger equation is given by

$$H(t)\Psi = i\hbar\partial_t\Psi, \tag{106}$$

where $H(t) = H_0 + H'(t)$, H_0 is time-independent Hamiltonian and $H'(t)$ is the approximated perturbed Hamiltonian in Eq. (104). We substitute the wave function in Eq. (105) into the time-dependent Schrodinger equation, then we have

$$\dot{c}_a(t) = -\frac{i}{\hbar}\left[c_a(t)H'_{aa} + H'_{ab}e^{-i\omega_{ba}t}c_b(t)\right], \tag{106}$$

$$\dot{c}_b(t) = -\frac{i}{\hbar}\left[c_b(t)H'_{bb} + H'_{ba}e^{i\omega_{ba}t}c_a(t)\right]. \tag{107}$$

The diagonal matrix elements of H' are zero, i.e. $H'_{aa} = H'_{bb} = 0$, which leads to

$$\dot{c}_a = -\frac{i}{\hbar} H'_{ab} e^{-i\omega_{ba}t} c_b, \tag{108}$$

$$\dot{c}_b = -\frac{i}{\hbar} H'_{ba} e^{i\omega_{ba}t} c_a. \tag{109}$$

Substituting the approximated potential into Eqs. (108) and (109), we have

$$\dot{c}_a = \frac{V_{ab}}{2\hbar} e^{-i\omega_{ba}t} e^{i\omega t} c_b, \tag{110}$$

$$\dot{c}_b = -\frac{V_{ba}}{2\hbar} e^{i\omega_{ba}t} e^{-i\omega t} c_a. \tag{111}$$

These equations are solved with the initial conditions:

$$c_a(0) = 1 \quad \text{and} \quad c_b(0) = 0. \tag{112}$$

Differentiating $\dot{c}_b$ in Eq. (111), we have

$$\ddot{c}_b = -\frac{V_{ba}}{2\hbar}\left[i(\omega_{ba} - \omega) e^{i(\omega_{ba}-\omega)t} c_a + e^{i(\omega_{ba}-\omega)t} \dot{c}_a\right]. \tag{113}$$

Substituting $\dot{c}_a$ in Eq. (110) into Eq. (113), we have

$$\begin{aligned} \ddot{c}_b &= i(\omega_{ba} - \omega)\left[-\frac{V_{ba}}{2\hbar} e^{i(\omega_{ba}-\omega)t} c_a\right] - \frac{V_{ba}}{2\hbar} e^{i(\omega_{ba}-\omega)t}\left[\frac{V_{ab}}{2\hbar} e^{-i(\omega_{ba}-\omega)t} c_b\right] \\ &= i(\omega_{ba} - \omega)\dot{c}_b - \frac{|V_{ab}|^2}{(2\hbar)^2} c_b. \end{aligned} \tag{114}$$

Then, we obtain the second order differential equation for c_b:

$$\frac{d^2 c_b}{dt^2} + i(\omega - \omega_{ba})\frac{dc_b}{dt} + \frac{|V_{ab}|^2}{(2\hbar)^2} c_b = 0 \tag{115}$$

The differential equation in Eq. (115) is a linear homogeneous differential equation, the solution is of the form $c_b = e^{\lambda t}$. Substituting $e^{\lambda t}$ into Eq. (115), we have

$$\lambda^2 e^{\lambda t} + i\lambda(\omega - \omega_{ba}) e^{\lambda t} + \frac{|V_{ab}|^2}{(2\hbar)^2} e^{\lambda t} = 0. \tag{116}$$

We obtain the characteristic equation for the parameter λ by Eliminating $e^{\lambda t}$ in Eq. (116):

$$\lambda^2 + i\lambda(\omega - \omega_{ba}) + \frac{|V_{ab}|^2}{(2\hbar)^2} = 0, \tag{117}$$

which has the solution:

$$\lambda = \frac{1}{2}\left[-i(\omega - \omega_{ba}) \pm \sqrt{-(\omega - \omega_{ba})^2 - \frac{|V_{ab}|^2}{\hbar^2}}\right] = i\left[-\frac{(\omega - \omega_{ba})}{2} \pm \omega_r\right],$$

where $\omega_r = \frac{1}{2}\sqrt{(\omega-\omega_{ba})^2 + \frac{|V_{ab}|^2}{\hbar^2}}$ is so-called the Rabi flopping frequency.

We obtain the general solution of c_b as:

$$c_b(t) = e^{-\frac{i(\omega-\omega_{ba})t}{2}}\left[\mathrm{A}\, e^{i\omega_r t} + \mathrm{B}\, e^{-i\omega_r t}\right], \tag{118}$$

$$= e^{-\frac{i(\omega-\omega_{ba})t}{2}}\left[\mathrm{A}\cos(\omega_r t) + \mathrm{B}\sin(\omega_r t)\right]. \tag{119}$$

The coefficient A and B are determined by the initial condition $c_b(0) = 0$, which leads to that A is zero. Thus the transition probability amplitude $\mathrm{c}_b(t)$ is given by

$$\mathrm{c}_b(t) = \mathrm{B}e^{-\frac{i(\omega-\omega_{ba})t}{2}}\sin(\omega_r t). \tag{120}$$

Taking the derivative of $\mathrm{c}_b(t)$ in Eq. (120) and substituting it into Eq. (111), we obtain the transition probability amplitude $c_a(t)$:

$$c_a(t) = \mathrm{B}\frac{2\hbar}{V_{ba}}e^{i(\omega-\omega_{ba})t/2}\left[-\omega_r\cos(\omega_r t) + \frac{i(\omega-\omega_{ba})}{2}\sin(\omega_r t)\right]. \tag{121}$$

The coefficient B in Eq. (121) is determined by the initial condition($c_a(0) = 1$,):

$$\mathrm{B} = -\frac{V_{ba}}{2\hbar\omega_r}. \tag{122}$$

Then, the general solution of the transition probability amplitude is:

$$c_a(t) = e^{i(\omega-\omega_{ba})t/2}\left[\cos(\omega_r t) - \frac{i(\omega-\omega_{ba})}{2\omega_r}\sin(\omega_r t)\right], \tag{123}$$

$$c_b(t) = -\frac{1}{2\hbar\omega_r}V_{ba}e^{i(\omega_{ba}-\omega)t/2}\sin(\omega_r t). \tag{124}$$

The transition probability of each state at time *t* is

$$P_a = |c_a(t)|^2 = \cos^2(\omega_r t) + \left|\frac{(\omega-\omega_{ba})}{2\omega_r}\right|^2\sin^2(\omega_r t), \tag{125}$$

$$P_b = |c_b(t)|^2 = \left|\frac{V_{ba}}{2\hbar\omega_r}\right|^2\sin^2(\omega_r t). \tag{126}$$

This results in Eq. (125) and Eq. (126) show that the transition probability has no linearity. The transition probability P_b derived from rotating wave approximation in Eq. (126) has a similar form to the transition probability derived from perturbation theory in Eq. (103), which implies that the rotating wave approximation is a good approximation when the driving

frequency is close to the transition frequency.

2.4 Strong-Field Approximation

When an intense laser pulse is irradiated in a system, the perturbation theory is no longer a good approximation for the system. The strong-field approximation (SFA) is a good approximation to calculate the ionization, when the laser field is dominant over the Coulomb potential.

Assume we apply an intense laser pulse to a system, there are two complete set of states Ψ_n and Φ_n in the system, respectively. The complete set of states Ψ_n that satisfy the time-dependent Schrodinger equation describing the atomic electron that has the interaction with an intense laser pulse

$$i\hbar\partial_t\Psi_n(t) = H(t)\Psi_n(t). \tag{127}$$

The other complete set of Φ_n that satisfy the Schrodinger equation describing an atomic electron that does not experience the laser pulse

$$i\hbar\partial_t\Phi_n = H_0\Phi_n. \tag{128}$$

The difference between the complete Hamiltonian and the non-perturbed Hamiltonian will vanish at both plus and minus infinity in time because the laser pulse is not present there

$$\lim_{t\to\pm\infty}[H(t) - H_0] = 0. \tag{129}$$

At minus infinity time, a one-to-one identification will be made between the elements of two complete set, so that the two complete sets are well-defined. After the laser interaction has occurred, the only way to find out what has happened is to take probability amplitude overlaps of all possible final states Φ_f with the state that began as a particular interacting state Ψ_i. This is so-called the *S*-matrix:

$$S_{fi} = \lim_{t\to+\infty}(\Phi_f, \Psi_i). \tag{130}$$

We subtract the amplitude that no interaction has occurred and denote that by M_{fi}:

$$M_{fi} \equiv (S_{fi} - 1) = \lim_{t\to+\infty}(\Phi_f, \Psi_i) - \lim_{t\to-\infty}(\Phi_f, \Psi_i), \tag{131}$$

or Eq. (131) can be also written as:

$$M_{fi} = \int_{-\infty}^{+\infty} dt \frac{\partial}{\partial t}(\Phi_f, \Psi_i). \tag{132}$$

We can use the time-dependent Schrodinger equation to remove the time derivatives in Eq. (132), then we have

$$M_{fi} = -\frac{i}{\hbar}\int_{-\infty}^{+\infty} dt \left(\Phi_f, H_I \Psi_i\right), \tag{133}$$

where $H_I \equiv H(t) - H_0$. This transition amplitude is so-called the direct time amplitude. An alternative form is so-called the time reversed amplitude:

$$M_{fi} = -\frac{i}{\hbar}\int_{-\infty}^{+\infty} dt \left(\Psi_f, H_I \Phi_i\right), \tag{134}$$

where the interacting state is the final state instead of the initial state. The direct time amplitude in Eq. (133) and the time reversed amplitude in Eq. (134) are equivalent. The difference between them is that instead of one-to-one identification are made between the elements of two complete set at minus infinity time, it is done at plus infinity time. The strong-field approximation is based on the time reversed amplitude in Eq. (134).

When an intense laser field is irradiated to a system, the eigenstates of non-perturbed Hamiltonian will be shifted by an intense laser. The shifted state is so-called "Volkov state". The transition amplitude is written as:

$$M_{fi} = -\frac{i}{\hbar}\int_{-\infty}^{+\infty} dt \left(\Psi_f^{\text{Volkov}}, H_I \Phi_i\right), \tag{135}$$

where the Volkov state is the final state, this makes SFA not exact.

2.5 Floquet Theory

When the time dependent Hamiltonian is periodic in time, the Floquet theory can be used as a method to obtain the solution of time dependent Schrodinger equation. In the following, we explain the Floquet theory to discuss a problem with a sinusoidal perturbed Hamiltonian.

We consider a system with the dependent Schrodinger equation given by

$$i\hbar\partial_t \Psi(t) = \hat{H}(t)\Psi(\vec{r}, t), \tag{136}$$

where the Hamiltonian $\widehat{H}(t)$ consist of the time-independent part $\widehat{H}_0$ and the time dependent part $\widehat{H}'(t)$.

The Hamiltonian is a periodic function in time:

$$\widehat{H}(t+T) = \widehat{H}(t). \tag{137}$$

Now we introduce the time evolution operator after one cycle of time. The differential equation for the time evolution operator is

$$i\hbar\partial_t U(t,t_0) = \widehat{H}(t)U(t,t_0), \tag{138}$$

with the initial condition $U(t_0,t_0) = I$. This equation is valid for any times t_0 and t. After one cycle of time, the differential equation of the time evolution operator is given by

$$i\hbar\partial_t U(t+T,t_0+T) = \widehat{H}(t+T)U(t+T,t_0+T), \tag{139}$$

Using Eq.(137), we also have

$$i\hbar\partial_t U(t+T,t_0+T) = \widehat{H}(t)U(t+T,t_0+T). \tag{140}$$

$U(t+T,t_0+T)$ and $U(t,t_0)$ satisfy the same linear differential equation (see Eqs. (138) and (140)) with the same initial condition, thus we have

$$U(t+T,t_0+T) = U(t,t_0), \tag{141}$$

which implies that the time evolution operator for many cycle of time is

$$U(t+nT,t) = [U(t+T,t)]^n. \tag{142}$$

Now we consider an eigen function $|\Psi_j^{\mathrm{F}}\rangle$ of the time evolution operator for one cycle with the corresponding eigenvalue λ

$$U(t+T,t)|\Psi_j^{\mathrm{F}}\rangle = \lambda_T|\Psi_j^{\mathrm{F}}\rangle. \tag{143}$$

From Eq. (142), we find that the corresponding evolution operator is

$$U(t+nT,t) = [U(t+T,t)]^n, \tag{144}$$

for any integer *n*. Equation(144) implies that any eigenvalue λ_{nT} of $U(t+nT,t)$ can be written in terms of an eigenvalue λ_T of $U(t+T,t)$

$$\lambda_{nT} = (\lambda_T)^n. \tag{145}$$

For an arbitrary number n, we have

$$U(t-nT,t)U(t+nT,t)=\lambda_{-nT}\lambda_{nT}=(\lambda_T)^{-n}(\lambda_T)^n=1. \tag{146}$$

From Eq. (146) and the conservation of probability, we find that the time evolution operator is unitary and λ_T is a complex number

$$\lambda_T=e^{-i\theta/\hbar}, \tag{147}$$

where θ is an arbitrary real number. Then, we have that

$$U(t+T,t)\left|\Psi_j^{\mathrm{F}}\right\rangle=e^{-i\theta/\hbar}\left|\Psi_j^{\mathrm{F}}\right\rangle, \tag{148}$$

where $\left|\Psi_j^{\mathrm{F}}\right\rangle$ is called the Floquet state. Assume we write the Floquet state in the form

$$\Psi_j^{\mathrm{F}}(t)=e^{-i\frac{\varepsilon_j}{\hbar}t}\phi_j(t), \tag{149}$$

where $\phi_j(t)$ is called quasi-state and ε_j is called the Floquet energy. In order to satisfy Eq.(148) for any t, $\phi_j(t)$ must be periodic in time with the same period as the Hamiltonian, namely

$$\phi_j(t+T)=\phi_j(t). \tag{150}$$

Here, the problem is how to obtain Floquet states. Once we obtain the Floquet states, the exact wave function is a linear combination of them

$$\Psi(t)=\sum_{j=0}^{\infty}f_j\Psi_j^{\mathrm{F}}(t), \tag{151}$$

where coefficient f_j can be determined by the initial condition. We are showing that the quasi-state $\phi_j(t)$ can be obtained by recasting the problem in the form of a time independent eigensystem. Since the quasi-state is periodic in time, it can be expanded in a Fourier series.

$$\phi_j(t)=\sum_{n=-\infty}^{\infty}c_n(\vec{r})e^{in\omega t}, \tag{152}$$

where $\omega=\frac{2\pi}{T}$. Besides, the coefficient $c_n(\vec{r})$ does not depend on time, we can expand the coefficient with a complete basis ψ_k of the time-independent Hamiltonian $\widehat{H}_0$

$$\phi_j(t)=\sum_{k}^{\infty}\sum_{n=-\infty}^{\infty}\alpha_{k,n}^{j}\,\psi_k\,e^{in\omega t}, \tag{153}$$

where the coefficient $\alpha_{k,n}^{j}$ is dependent on the laser intensity. Then, the Floquet state in Eq. (149) is given by

$$\Psi_j^{\mathrm{F}}(t) = \sum_{k}^{\infty} \sum_{n=-\infty}^{\infty} \alpha_{k,n}^{j}\, \psi_k\, e^{-\frac{i}{\hbar}(\varepsilon_j - n\hbar\omega)t}. \tag{154}$$

According to the Floquet theory, it shows that the origin eigenstates of time-independent Hamiltonian are coupled together to form Floquet states by a periodic potential. In other words, the eigenstate picture is transformed into the Floquet picture by a periodic potential. Then, the exact wave function is a linear combination of the Floquet states instead of the origin eigenstates. In experiments, we use the laser pulse as the interaction Hamiltonain. The duration of laser pulse is assumed to be sufficiently long so that the laser field can be approximated by a monochromatic field. By this kind of pulse, we can use the Floquet theory to analyze the system. Furthermore, the laser pulse with long duration increases gradually, so the transition is an adiabatic process. That means that the eigenstates are transformed to a Floquet state during the laser pulse is on, and the Floquet state is transformed back to the eigenstates with no transition at the end of laser pulse. In the following, we use the Floquet theory to discuss a system with a sinusoidal perturbed Hamiltonian.

Assume the electric field is a sinusoidal function of time and polarized along the *z* direction

$$\vec{E} = E_0 \sin(\omega t)\, \hat{k}. \tag{155}$$

The perturbed Hamiltonian is:

$$H' = -qzE_0 \sin(\omega t), \tag{156}$$

where q is the charge of the electron. According to the first order perturbation theory, the transition probability amplitude of each state is

$$T_m = \int_{t_i}^{t_f} \left\langle \Psi(\vec{r}, t) \middle| H' \middle| \psi_m e^{-i\frac{E_m}{\hbar}t} \right\rangle dt. \tag{157}$$

We use the strong field approximation in transition amplitude,

$$T_m = \sum_{j=0}^{\infty} f_j \int_{t_i}^{t_f} \left\langle \Psi_j^{\mathrm{F}}(t) \middle| H' \middle| \psi_m e^{-i\frac{E_m}{\hbar}t} \right\rangle dt, \tag{158}$$

where the final state is Floquet state instead of Volkov state. We substitute the Floquet state in Eq. (158) and factor the constant out, we have

$$T_m = \sum_{k}^{\infty} \sum_{n=-\infty}^{\infty} f_j \alpha_{k,n}^{j} \langle \psi_k | z | \psi_m \rangle \int_{-\infty}^{\infty} e^{-\frac{i}{\hbar}(\varepsilon_j - n\hbar\omega)t} \sin(\omega t) e^{-i\frac{E_m}{\hbar}t} \, dt. \tag{159}$$

The integral in Eq.(159) has none zero value only if

$$\varepsilon_j + n\hbar\omega - E_m = 0, \quad (n = -\infty \ldots 0,1,2 \ldots \infty). \tag{160}$$

This result shows that the transition takes place only if the photon energy satisfies the resonance condition, which is

$$\hbar\omega = \Delta E = \varepsilon_j + n\hbar\omega - E_m. \tag{161}$$

III. Results & Discussion

In this study we take a hydrogen atom as example to discuss the excitation process by intense laser field. Here we included the eigenstates of unperturbed hydrogen atom with the principle quantum numbers smaller than 3-1. First we examine the intensity dependence of the excitation probability with a single Gaussian laser pulse, which electric field is given by 1.8×10^{13} W/cm^2~7.1×10^{14} W/cm^2 with λ=800nm and duration is 40fs. The Schrodinger equation is solved by the Runge-Kutta method with the initial condition $\Psi(t)=\psi_0$ at t_i= -3,000 (a.u.) to obtain the transition probability at the final time t_f = 3,000 (a.u.). In Fig. 6 the transition probabilities are plotted as functions of the laser intensity in a log-log scale. Here the laser intensity is taken from 1.8×10^{13} W/cm^2 to 7.14×10^{14} W/cm^2. The transition probabilities show power dependences on the laser intensity with large values of the slope, and they can be classified into two groups having the slopes 9 and 10, respectively (The curves I^9 and I^{10} are also plotted in the figure for comparison.). The group having the slope of 9 includes 3s, 3d, 4s, 4d, 5s, 5d and 5g whereas the other group with the slope of 10 includes 2s, 2p, 3p, 3f, 4p, 4f and 5f. The slopes may indicate the number of photons involved in the transitions. It should be noted here that the transition energy is not necessarily equal to the photon energy times the number of photon. Actually even the smaller slope 9 leads to the energy $n\hbar\omega$ ~14 eV, which is larger than the ionization potential IP = 13.6 eV. Above mentioned tendencies observed in our calculation are very similar to the results for the oxygen molecular targets showing two slopes of 9 and 11. In the present result shows an interesting tendency in the members of groups. Except the 2s state, all the even (odd) states belong to the group with the slope 9 (10). In other words, the slope can be determined by the parity of the angular momentum. In order to discuss how the slope is related with the parity, we examine the transition dynamics in detail in the followings.

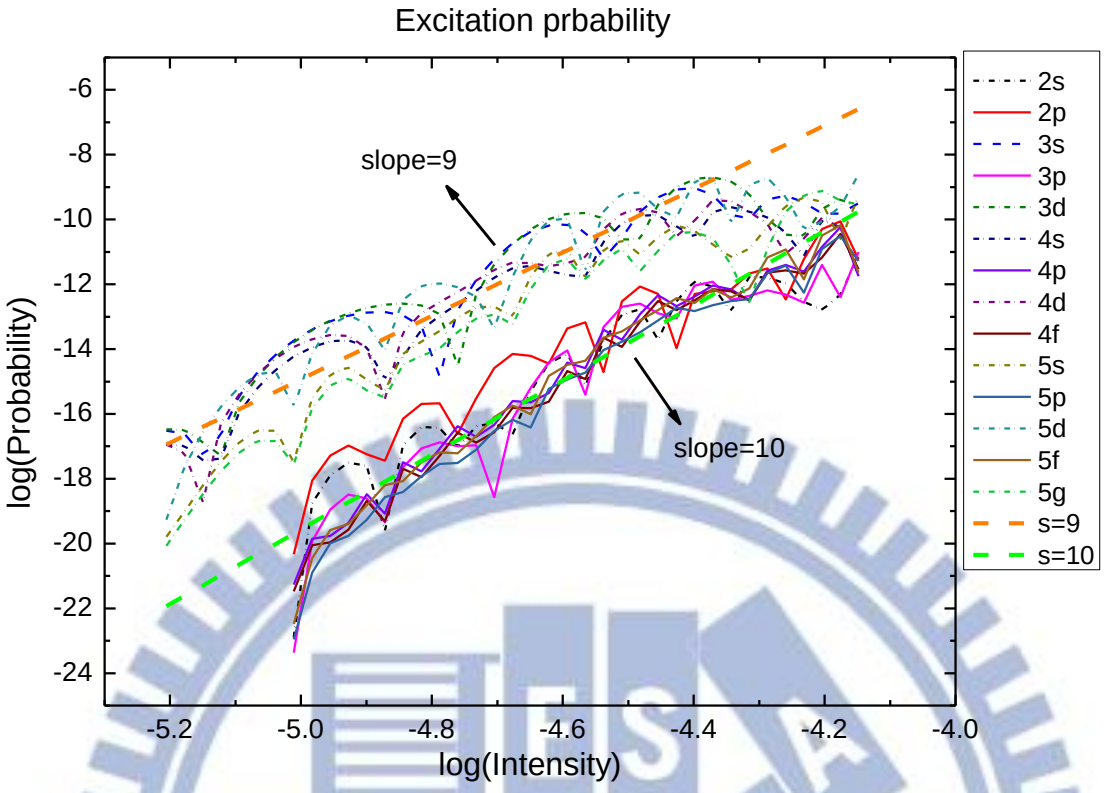

Figure 3-1 Excitation probabilities to the excited states (n<6) of hydrogen atom as functions of the laser intensity. Thick dashed lines are curves of I^9 and I^10.

Since the final transition probability does not provide the information on what happens during the transition, we have to consider the probability amplitude $c_k(t)$ as function of time, which is shown in Fig. 3-2. As is shown in the figure, the transition amplitudes have very complicated time dependence. They show maximum at t=0, and they are significantly larger than the transition amplitudes at the final time. It should be noted here that many states have too small transition amplitudes to be seen in the plot. We observe the same behavior if you magnify each of them. This implies that the transition mechanism is not simple resonance one photon transition, which shows monotonically increasing probabilities as a function of time.

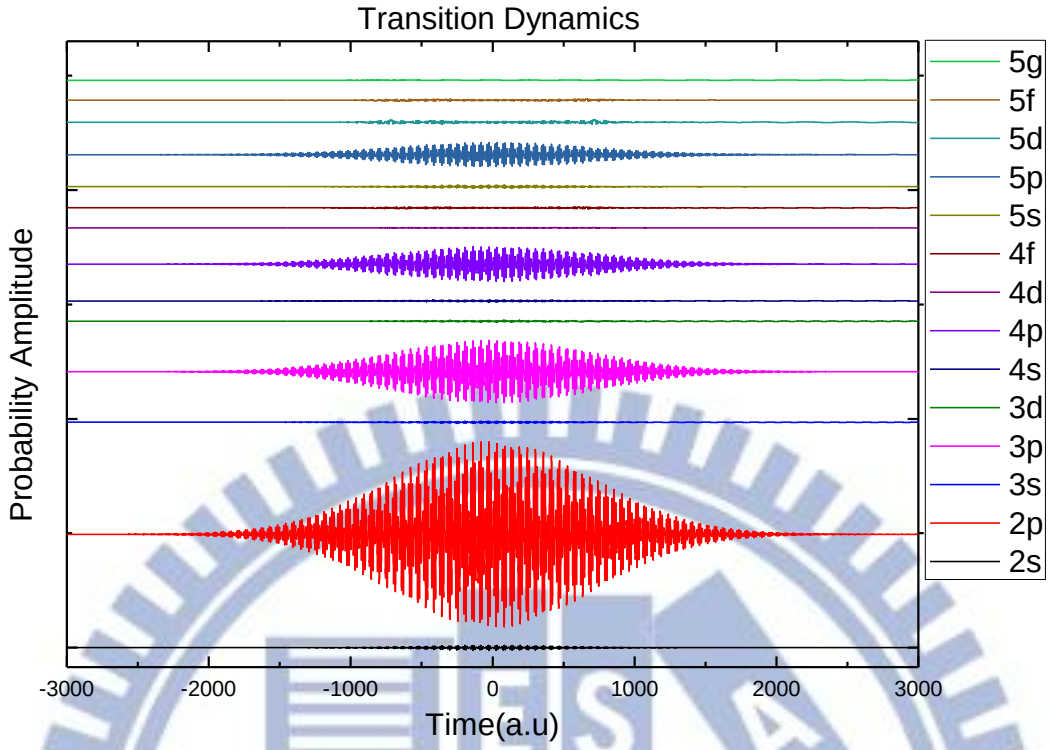

Figure 3-2 Excitation probability amplitude of excited states from - 3,000 (a.u.) to 3000 (a.u.). Here, we shows the real part of excitation probability amplitude.

In order to analyze such complicated behavior, we utilize the Floquet theorem introduced in Chapter (II). According to the Floquet theorem, the time dependent wave function has the form

$$\Psi(t) = \sum_{j=0}^{\infty} f_j \sum_{k}^{\infty} \sum_{n=-\infty}^{\infty} \alpha_{k,n}^{j}\, \psi_k\, e^{-\frac{i}{\hbar}(\varepsilon_j - n\hbar\omega)t}, \qquad (162)$$

which can also be rewritten using the probability amplitudes as

$$\Psi(t) = \sum_{k}^{\infty} c_k(t)\, \psi_k. \qquad (163)$$

Comparing Eq.(162) and Eq.(163), we obtain

$$c_k(t) = \sum_{n=-\infty}^{\infty} \sum_{j=0}^{\infty} f_j\, \alpha_{k,n}^{j} e^{-\frac{i}{\hbar}(\varepsilon_j - n\hbar\omega)t} \qquad (164)$$

which implies that the transition amplitudes are linear combination of periodic functions in

time. We can thus Fourier transform $c_k(t)$ into the frequency domain $c_k(\omega)$, which peaks tell us the quasi energy ε_j and the coefficients f_j and $\alpha_{k,n}^{j}$. Since our laser filed is a pulse (not periodic in time), the Floquet theorem is applicable only in an adiabatic way. We can define the Floquet states at a moment with a constant intensity, which we call the adiabatic Floquet states. If the intensity change in time is sufficiently slow, the system follows the same adiabatic Floquet states in its time propagation. This is the adiabatic approximation for the Floquet states [15][16]. Now let's consider what happens if the adiabatic approximation completely holds. At the initial time, when the laser field is off, the initial eigenstate can be regarded as the Floquet state with zero intensity. This Floquet state propagates in time following the adiabatic Floquet state. When the laser is on, the adiabatic Floquet state is a linear combination of the ground state as well as the excited states. This leads to the transient nonzero transition amplitudes, which is seen in Fig. 3-2 at t =0. After the laser is turned off, however, these transient transition amplitudes vanish, because the adiabatic Floquet state should be the initial eigenstate at the zero field limit. Thus the nonzero transition amplitude at the final time in Fig. 3-2 can be regarded as the nonadiabatic effect.

In order to discuss the nonadiabatic effect, we calculated the transition amplitudes with the laser pulse given by

$$\hat{E}(t) = \begin{cases} E_0 \sin(\omega t)\, e^{\frac{-t^2}{\tau^2}} & -3000 \le t \le 0 \\ E_0 \sin(\omega t) & 0 \le t \le \alpha \\ E_0 \sin[(\omega-\alpha)t]\, e^{\left[\frac{-(\omega-\alpha)t^2}{\tau^2}\right]} & \alpha \le t \le 3000 \end{cases}$$

, where $E_0, \omega, \tau, \alpha$ are 1.4×10^{14} W/cm^2, 800 nm, 1000 and 4100 respectively.

Here, with the use of this shape of the laser pulse, we can analyze the wave function with the use of the Floquet state, because the laser field is periodic during the intensity is kept constant. We hence Fourier transformed $c_k(t)$ in the limited time domain when the laser field is periodic. We can discuss the adiabatic Floquet states and their nonadibatic effect from the Floquet coefficients and quasi energies obtained in this way. The results are shown in Fig. 3-3.

Figure 3-3(a) shows $|c_k\ (\omega)|$ (k=1,2,,,15) as functions of ω. Here we displayed the vertical grid lines with the spacing 0.05703 in the atomic unit (equal to the optical frequency of our laser field). We find that there is only one dominant peak on $|c_1\ (\omega)|$ (k=1 corresponds to the ground state) at $\omega \approx 0.5$. This means that the wave function during the time interval mostly consists of only the unperturbed ground state. In other words, the wave function consists mainly of one Floquet state that is nearly equal to the initial eigenstate. This Floquet state is the one adiabatically propagated from the initial eigenstate. In Fig. 3-3(a)the peaks on the excited states are too small to be seen. In order to investigate these peaks in the excited states, we normalized each $|c_k\ (\omega)|$ so as that $\int_{-\infty}^{+\infty}|c_k\ (\omega)|\,d\omega = 1$. The normalized results are shown in Fig. 3-3(b). We observe that many peaks are localized in two regions: $0.342 < \omega < 0.684$ and $0 < \omega < 0.228$. All the peaks in the region $0.342 < \omega < 0.684$ have the positions at about 0.39, 0.44, 0.5, 0.56, and 0.61. These positions differ by the optical frequency. Note that two peaks belonging to the same Floquet state should have the positions differ by the optical frequency times an integer. This is because Eq. (164) imply that such two peaks have a common quasi energy. We conclude that these peaks belong to the same Floquet state. Since this Floquet state includes the peak at $\omega = 0.5$ on 1s state (the peak seen in the unnormalized result Fig 3-3(a)), it is the adiabatic Floquet state originated from the 1s eigenstate. We can clearly see the excited state components of this Floquet state in Fig. 3-3(b). One interesting feature here is that the peaks in this Floquet state has parity dependence. All the odd angular momentum states has the peaks at 0.44 and 0.56 (odd states are in solid lines), whereas the even states peak at 0.39, 0.5, 0.61 (dotted lines). Other peaks at a position satisfying $0.5 + n\omega$ (For example, the peak on 4f state at $\omega = 0.33$) also belong to the same Floquet state. The peaks in the region $0 < \omega < 0.228$, on the other hand, does not belong to the Floquet state discussed above because the positions are not at $0.5 + n\omega$. Thus these peaks belong to the Floquet states populated after the nonadiabatic transition from the initial Floquet

state.

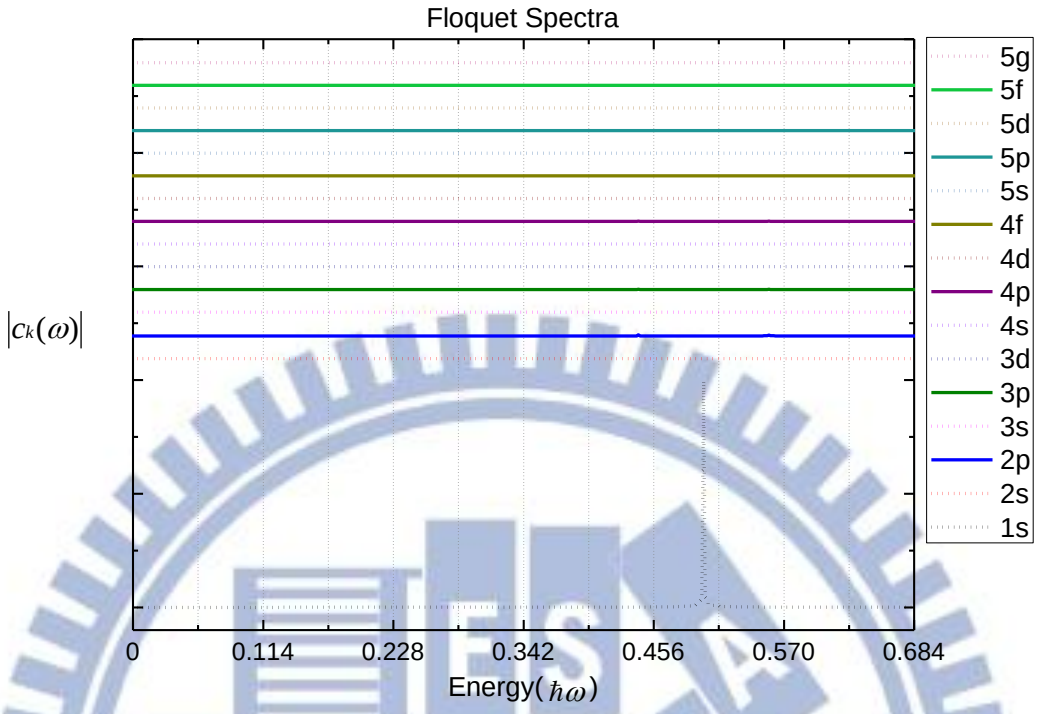

Figure 3-3(a) Fourier transform the excitation probability amplitudes into frequency domain. Floquet spectra is associated with the initial state is ground state.

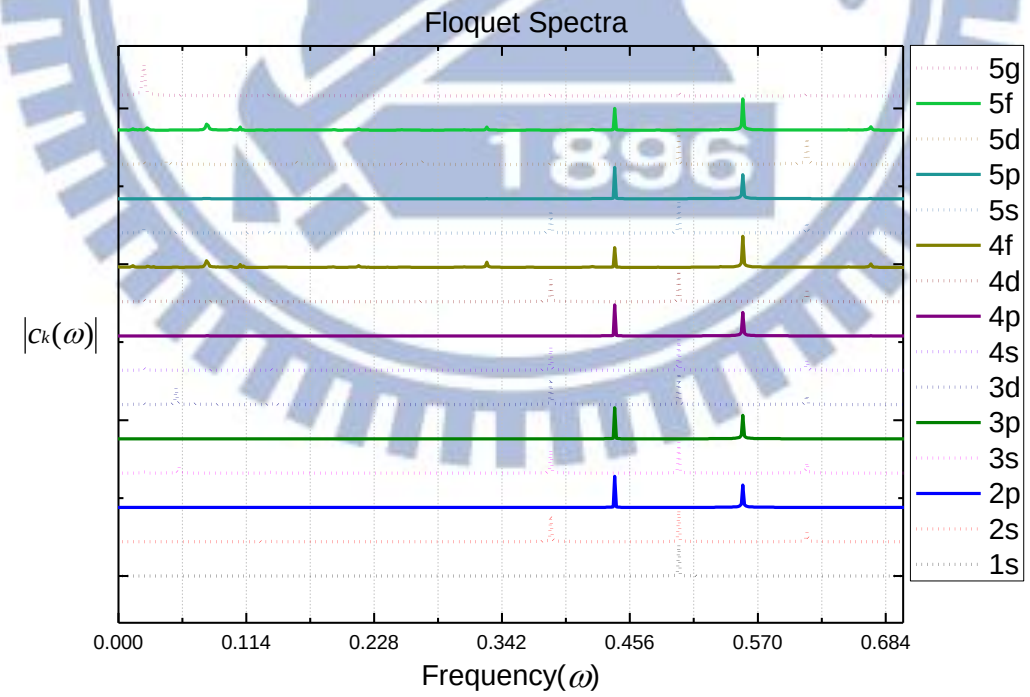

Figure 3-3(b) Normalized the result in Fig. 3-3(a) by $\int_{-\infty}^{+\infty}|c_k\ (\omega)|\,d\omega = 1$

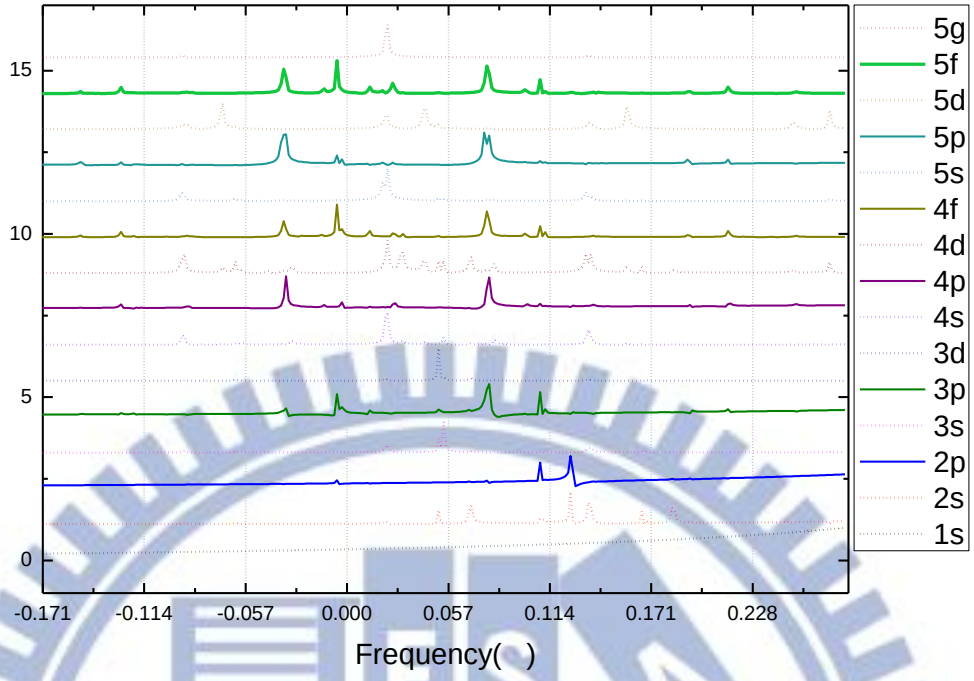

Figure 3-3(c) Magnify the normalized result in the region $-0.171 < \omega < 0.228$ in Fig. 3-3(b.)

In order to examine the nonadiabatically populated Floquet state, we focus on the region $-0.171 < \omega < 0.228$ (Fig 3-3(c)). Here we normalized the amplitudes according to the normalization condition $\int_{-0.171}^{0.228} |c_k(\omega)|\, d\omega = 1$. In this region we observe many Floquet states are involved, but we still see some parity dependence. For example, the peaks in the region $0.0 < \omega < 0.057$ are mainly on the even angular momentum states. As we mentioned above the final transition probabilities are attributed to the nonadiabatic transition. Fig 3-3(c) shows the information on the Floquet states nonadiabatically populated. We do not know, however, these Floquet states converge to which eigenstates as the final states. In order to discuss this, we have to understand the correlation between the eigenstates and Floquet states. For this purpose we performed essentially the same calculations as in Fig.3-3, but replacing the initial state from the ground state to varisous excited states.

In Figs. 3-4(a)~3-4(n), we show the Fourier transformed probability amplitudes as functions of the frequency with the initial states 2s-5g, respectively. We found that the peaks on the

even angular momentum eigenstatas (dotted lines) in the region $0.0 < \omega < 0.057$ exist only when the even angular momentum states are taken as the initial states (Figs. 3-4(a), 3-4(c), 3-4(e), 3-4(f), 3-4(h), 3-4(j), 3-4(l), and 3-4(n)). The peaks on odd eigenstates (solid lines), on the other hand, exist only in the case of odd angular momentum initial states in this region (Figs. 3-4(b), 3-4(d), 3-4(g), 3-4(i), 3-4(k), and 3-4(m)). This means that one we find peaks on even (odd) angular momentum states on a Floquet state, it converges to even (odd) eigenstate as the final state when the laser is turned off. As we discussed in Fig.3-3(c), the Floquet states nonadiabatically populated from the ground states have peaks mostly on the even angular momemntum states (dotted lines in Fig.3-3(c)) in this region. This means that these nonadiabatically populated Floquet states mostly converge into even angular momentum eigenstates as the final states. In Fig. 3-3(c) in this region, small peaks exist on odd angular momentum states (solid line), This small population leads to the transition to the odd angular momentum final states. This is basically why the transition probability to even states are larger than those to odd states by orders (see Fig. 3-1). In some cases we observe several peaks in one optical frequency (one vertical grid) as is seen in Fig.3-4(n) for example, which indicates more than one Floquet states are populated due to the nonadiabatic transitions between Floquet. The analysis of the parity of peaks in the region $0.0 < \omega < 0.057$ shows that the nonadiabatic transitions take places only between the states converging to the same parity states.

We have found that present Fourier-Floquet analysis of the transition amplitudes provides fruitful information on the non-perturbative exciation dynamics with the intense laser field. In what follows we propose a detailed excitation mechanism using the knowledge obtained so far:

(1) At the initial time, the atom is in the ground state with the laser turned off. When the laser is off, an eigenstate can be regarded as a Floquet state.

(2) As the intensity increases, the system propagates in time following mostly the adiabatic Floquet state associated with the initial state. There is a small nonadiabatic transition between the Floquet states, though.

(3) The adiabatic Floquet state associated with the initial state is a linear combinations of the ground and the excited states as shown in the range $0.342 < \omega < 0.684$ of the Fig. 3-3(b). The excited state components give rise to the large transient amplitude near the peak time (t=0) in Fig. 3-2. These amplitudes vanish when the laser is turned off as the Floquet state follows the adiabatic state converging to the ground state.

(4) The nonzero transition amplitude on the excited states at the final time, thus, are attributed to the nonadiabatic transitions to other Floquet states, which spectra is observed in the region $0 < \omega < 0.228$ of Fig. 3-3(b). Nonaidiabatic transitions between the Floquet states dominantly take places between those converging to the same parity eigen states when the laser is turned off. Since the ground state is an even angular momentum state, most of the Floquet states seen in this region converge to the even angular momentum eigenstates when the laser is turned off. Due to the nonadiabatic transitions between the even parity states, excited states populations may be redistributed among them, which can explain the reason for the same slopes in most of the even states. This is how the excitation to the even angular momentum state take place.

(5) Since the nonadiabatic transitions between different parity states hardly occur, the excitation to the odd angular momentum states have small probabilities compared to the even states. Similar to the even angular momentum states, nonadiabatic transitions between the odd states lead to the common slope for the odd states.

Above discussion does not explain why the slope is 9 and 10 for even and odd states respectively. This may be understood by considering this problem by using the strong field

approximation together with the information on the Floquet states obtained in this study. This, however, may be investigated in a near future.

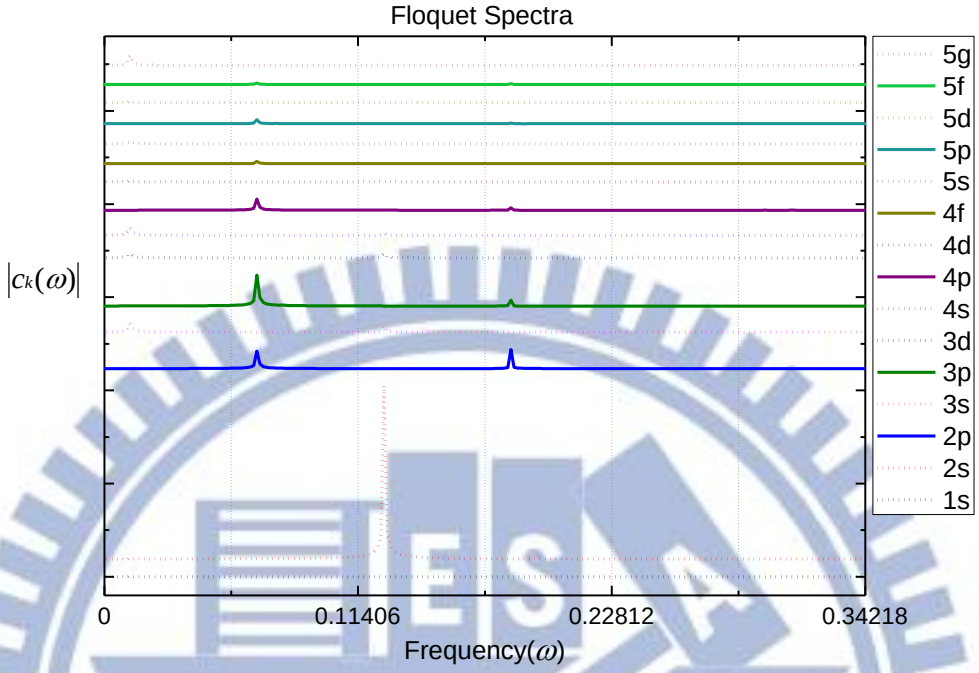

Figure 3-4(a) Fourier transform the excitation probability amplitude into frequency domain. This Floquet spectrum is associated with the initial state is1st excited state(2s).

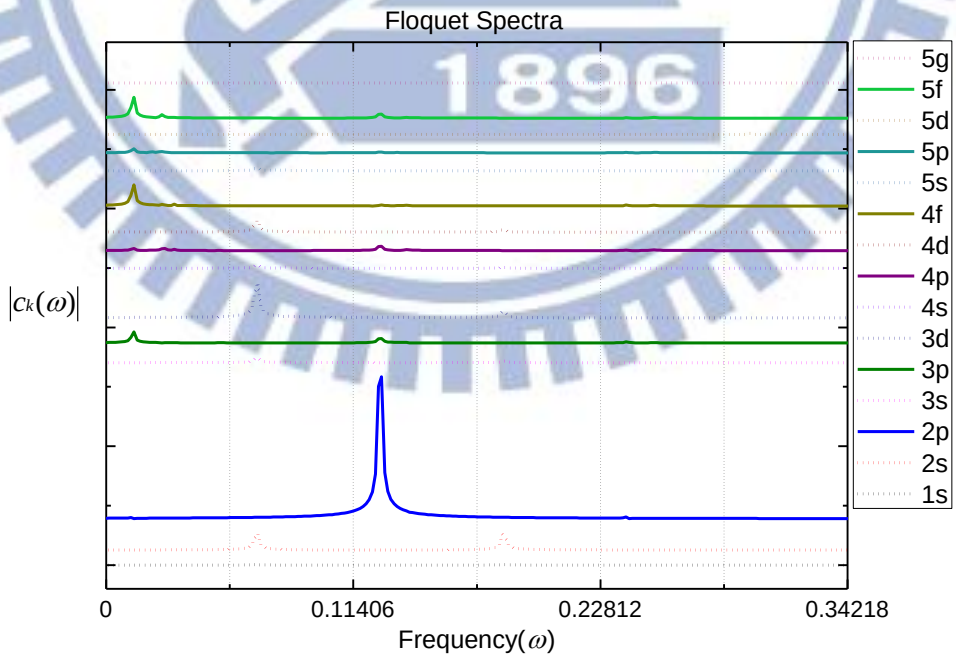

Figure 3-4(b) Fourier transform the excitation probability amplitude into frequency domain. This Floquet spectrum is associated with the initial state is 2nd excited state(2p).

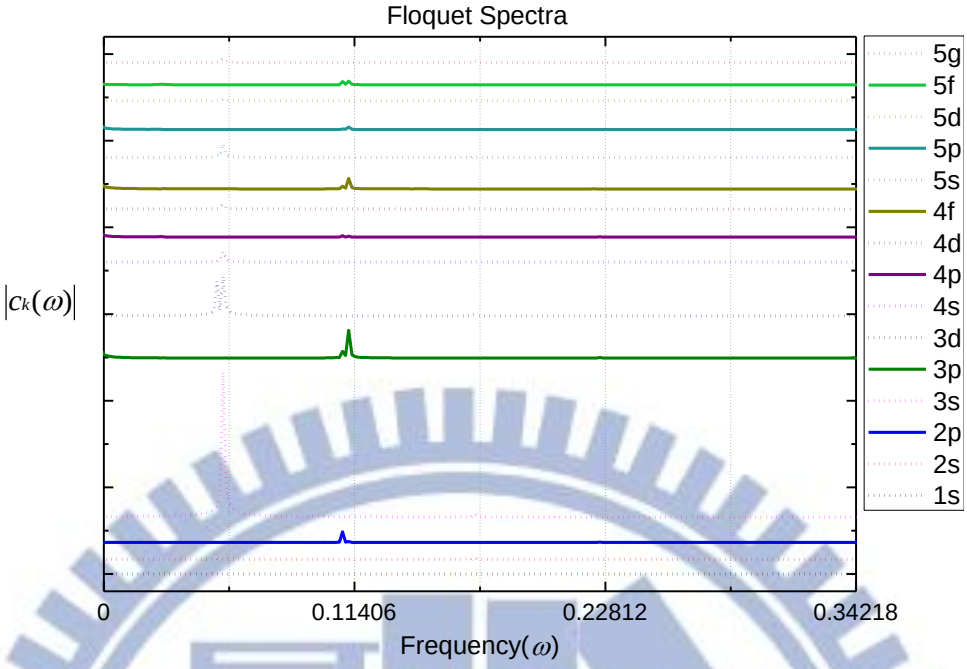

Figure 3-4(c) Fourier transform the excitation probability amplitude into frequency domain. This Floquet spectrum is associated with the initial state is 3rd excited state(3s).

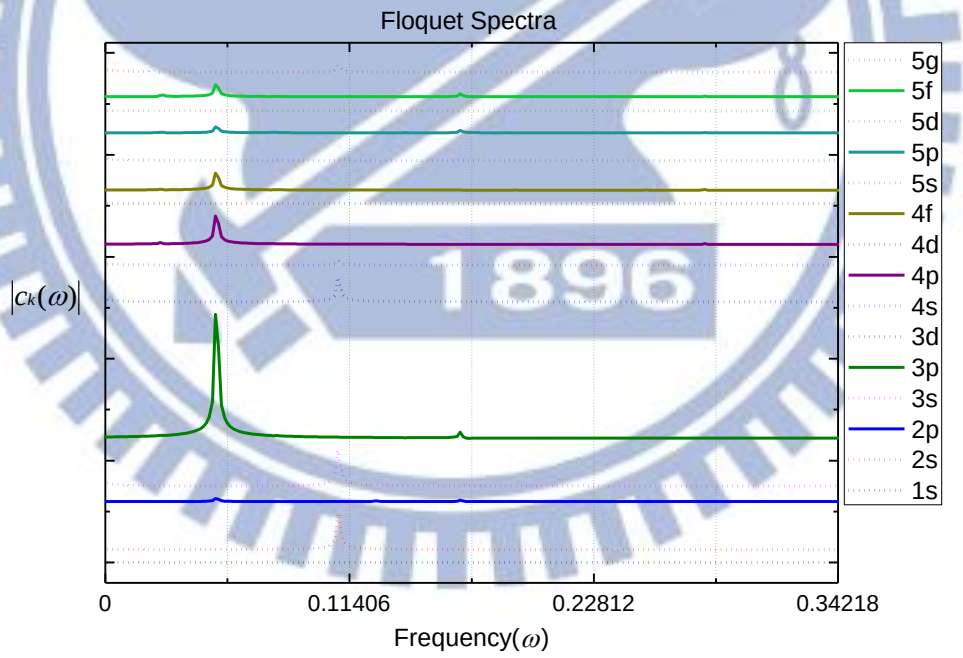

Figure 3-4(d) Fourier transform the excitation probability amplitude into frequency domain. This Floquet spectrum is associated with the initial state is 4th excited state(3p).

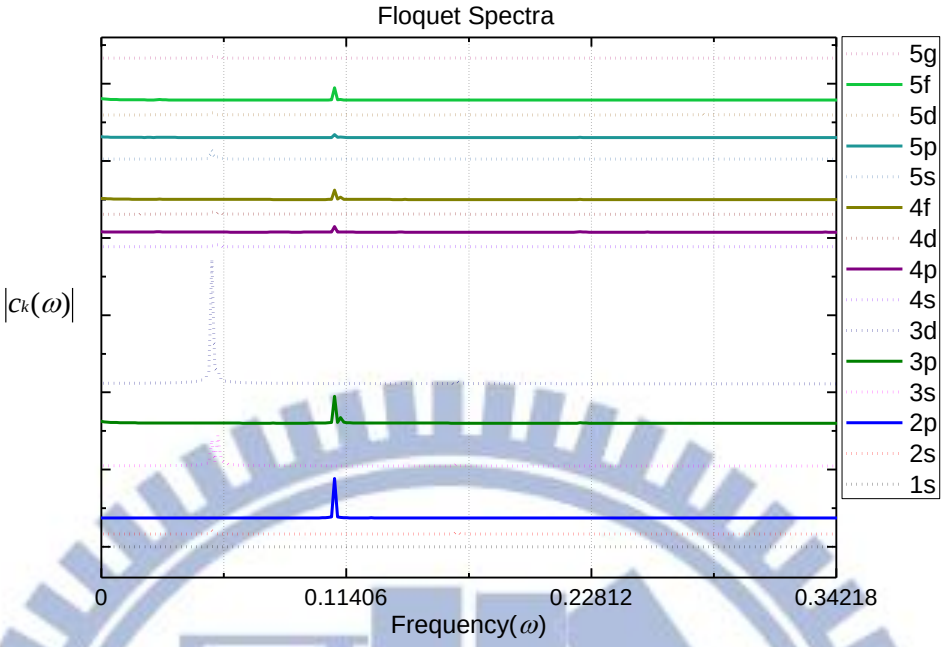

Figure 3-4(e) Fourier transform the excitation probability amplitude into frequency domain. This Floquet spectrum is associated with the initial state is 5th excited state(3d).

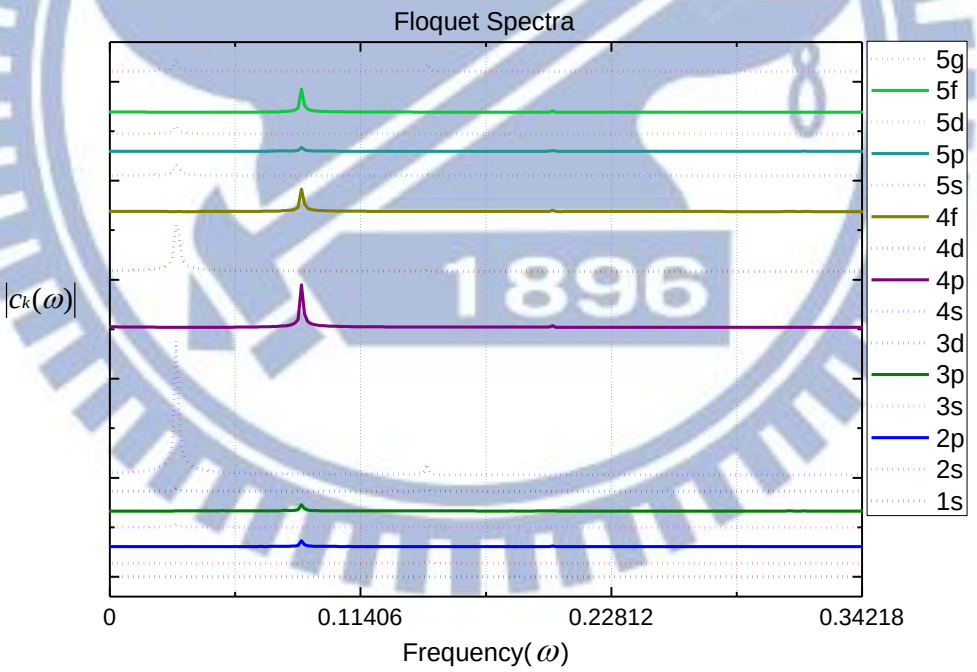

Figure 3-4(f) Fourier transform the excitation probability amplitude into frequency domain. This Floquet spectrum is associated with the initial state is 6th excited state(4s).

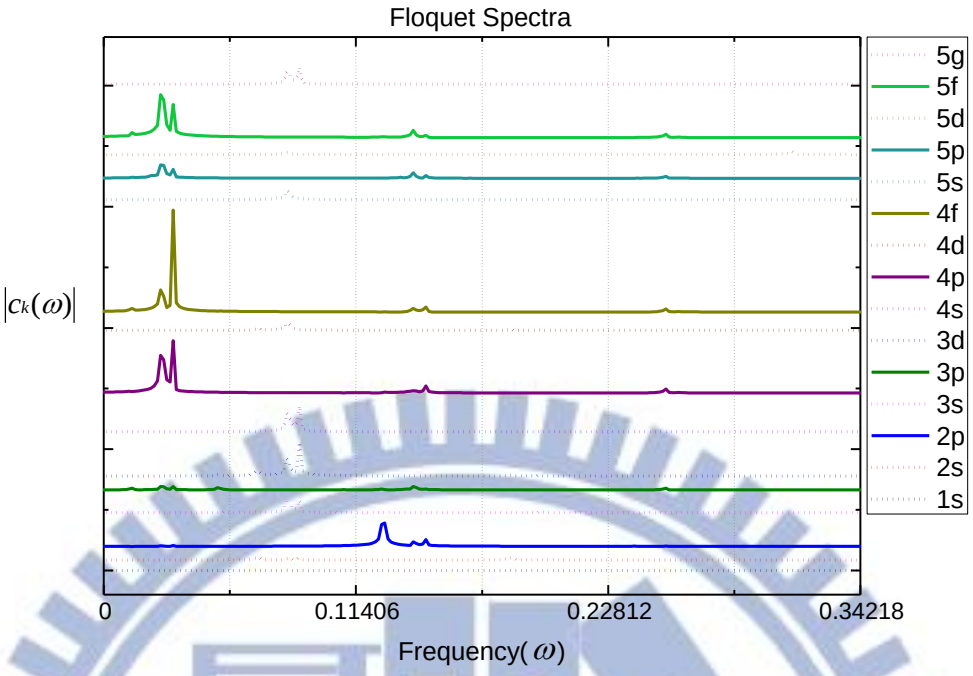

Figure 3-4(g) Fourier transform the excitation probability amplitude into frequency domain. This Floquet spectrum is associated with the initial state is 7th excited state(4p).

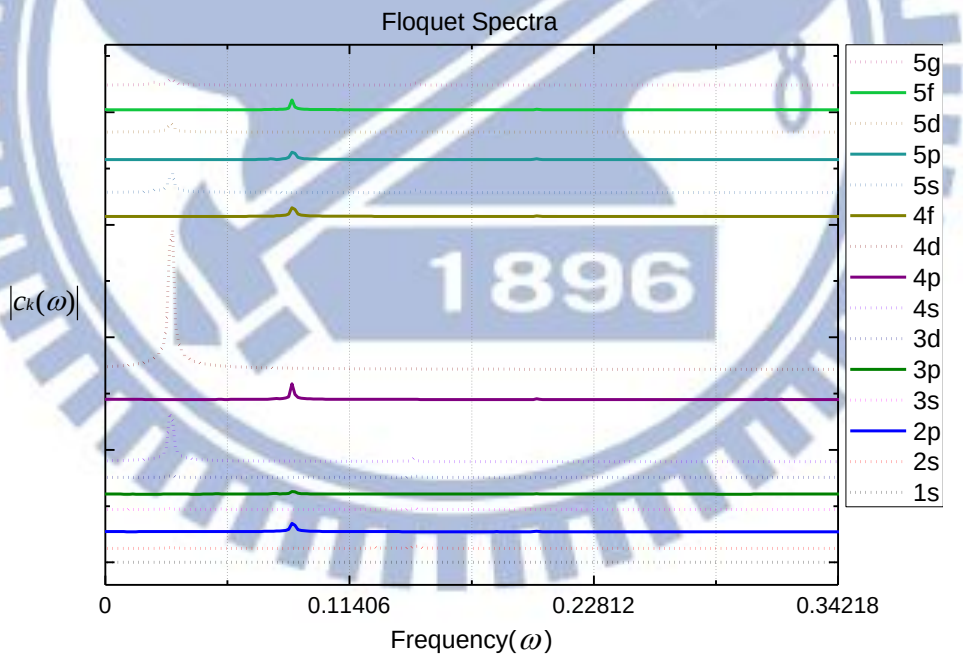

Figure 3-4(h) Fourier transform the excitation probability amplitude into frequency domain. This Floquet spectrum is associated with the initial state is 8th excited state(4d).

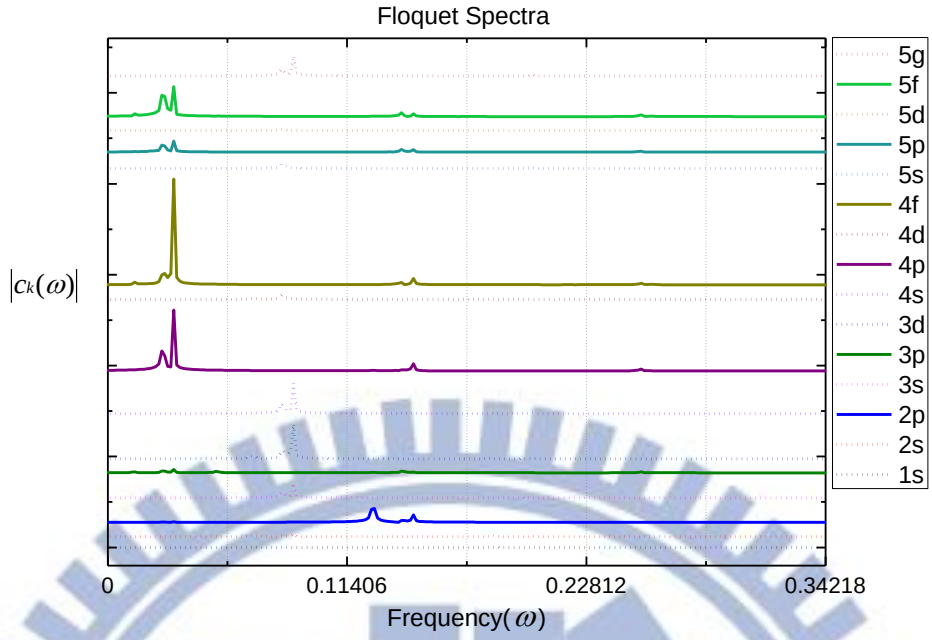

Figure 3-4(i) Fourier transform the excitation probability amplitude into frequency domain.This Floquet spectrum is associated with the initial state is 9th excited state(4f).

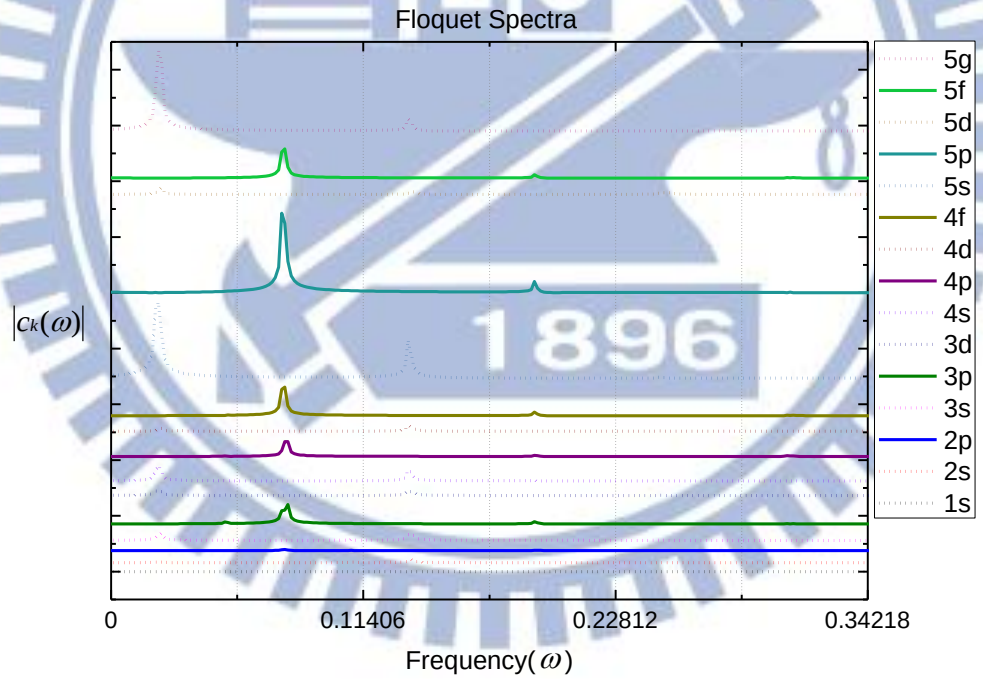

Figure 3-4(j) Fourier transform the excitation probability amplitude into frequency domain. This Floquet spectrum is associated with the initial state is 10th excited state(5s).

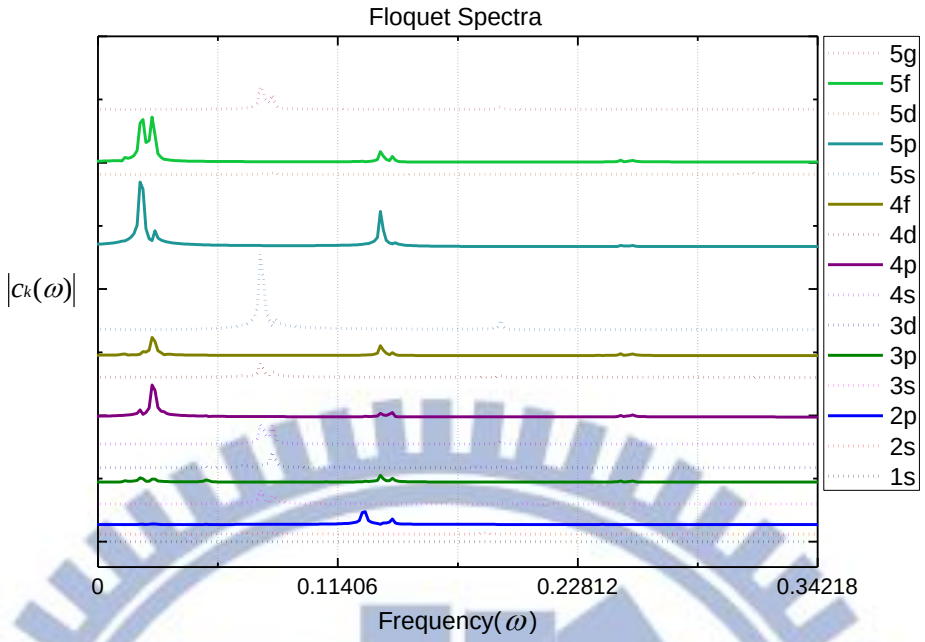

Figure 3-4(k) Fourier transform the excitation probability amplitude into frequency domain. This Floquet spectrum is associated with the initial state is 11th excited state(5p).

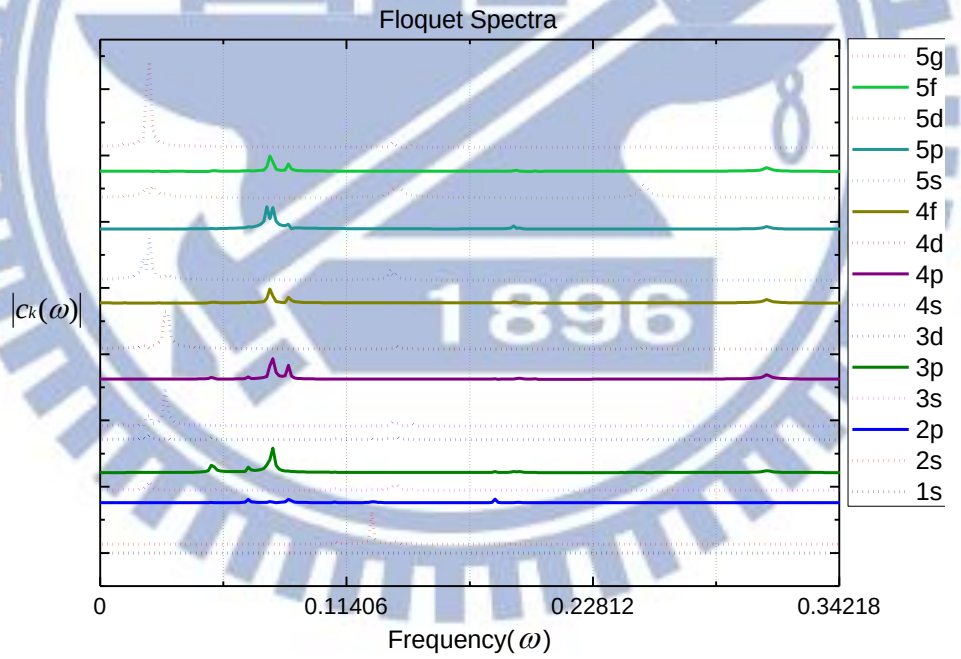

Figure 3-4(l) Fourier transform the excitation probability amplitude into frequency domain. This Floquet spectrum is associated with the initial state is 12th excited state(5d).

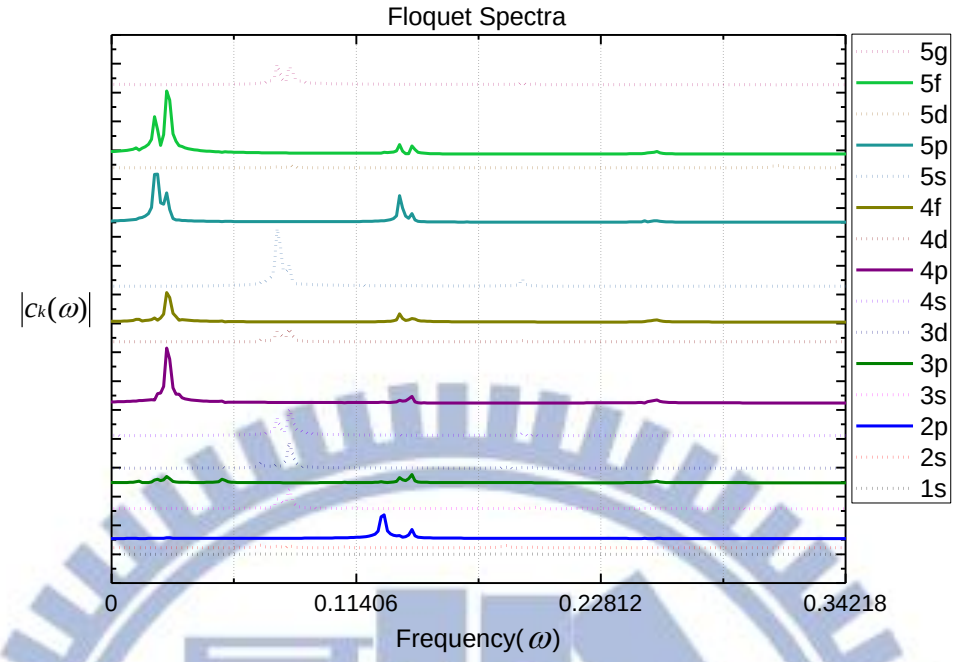

Figure 3-4(m) Fourier transform the excitation probability amplitude into frequency domain. This Floquet spectrum is associated with the initial state is 13th excited state(5f).

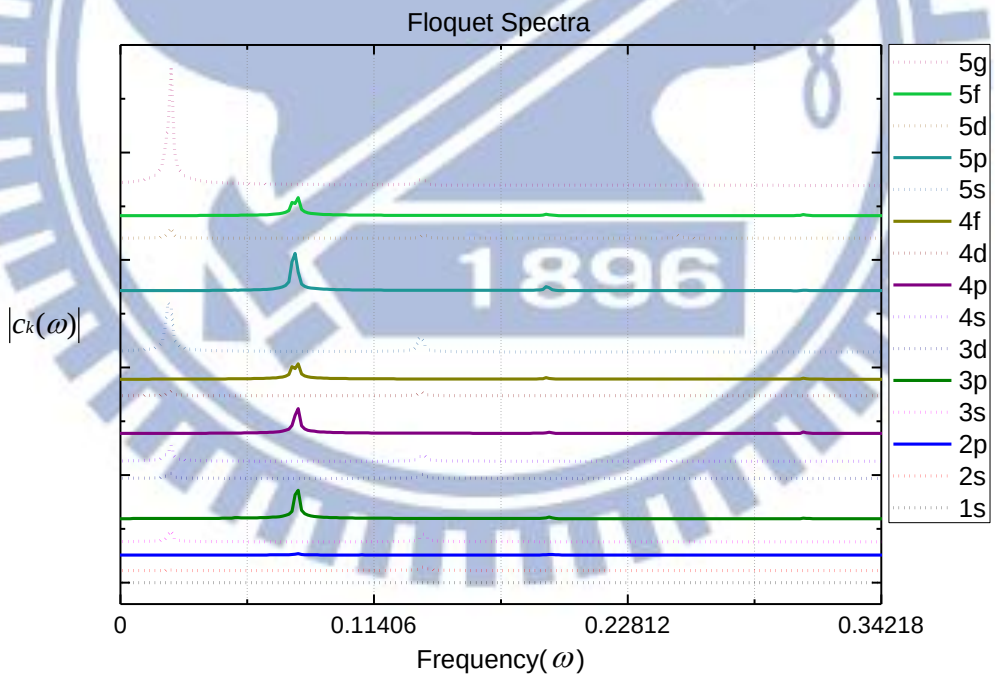

Figure 3-4(n) Fourier transform the excitation probability amplitude into frequency domain. This Floquet spectrum is associated with the initial state is 14th excited state(5g).

In the experiments, they use molecules as target. As is explained in the introduction, they measure the fluorescence signals from the fragments. The fluorescence signals are attributed

to three physical processes: First nonlinear excitation by intense femto second laser populate various excited states as we discussed through the thesis. After that some of the excited states dissociate into fragments in electronically excited states. Since highly excited states are populated, dissociation process involves a breakdown of the Born-Oppenheimer approximation. A fragment in an excited state can emit a photon to be de-excited to a lower state. If it is de-excited to a fluorescing state, it may emit another photon. This kind of series of photon emission is called cascade fluorescence. In this thesis we focus on the excitation process, but our results cannot directly be compared with the experimental results without the analysis of dissociation and cascading processes, which is beyond the scope of us. Here we propose a new experimental scheme for the direct observation of the excited states in the parent molecule. The basic idea is similar to so called Ramsey fringes. Hereafter we briefly explain basic idea of it:

We consider the transition probabilities induced by a double weak pulse with the time delay *T*. Each pulse are polarized along z direction having the carrier frequency ω. The perturbed Hamiltonian is given by

$$H'(\vec{r},t) = V'_1(\vec{r},t) + V_2(\vec{r},t), \tag{165}$$

with $V_1(\vec{r},t) = zE_0\sin(\omega t)e^{-t^2/\tau^2}$ and $V_2(\vec{r},t) = zE_0\sin[\omega(t+T)]e^{-(t+T)^2/\tau^2}$. Here we assume that E_0 is sufficiently weak. Using the first-order perturbation theory, the transition amplitude from the initial state $|i\rangle$ to a final state $|n\rangle$ by the first and the second pulses are respectively given by

$$\begin{aligned} c_{n1} &\cong \int_{-\infty}^{+\infty} dt' e^{i\omega_{ni}t'} \langle n|V_1(t')|i\rangle \\ &\cong \int_{-\infty}^{+\infty} dt' \langle n|z|i\rangle E_0\sin[\omega t']e^{-\frac{t'^2}{\tau^2}}e^{i\omega_{ni}t'}. \end{aligned} \tag{166}$$

and

$$c_{n2} \cong \int_{-\infty}^{+\infty} dt' e^{i\omega_{ni}t'} \langle n|V_2(t')|i\rangle \tag{167}$$

$$\cong \int_{-\infty}^{+\infty} dt' \langle n|z|i\rangle E_0 \sin[\omega(t'+T)] e^{-\frac{(t'+T)^2}{\tau^2}} e^{i\omega_{ni}t'}. \qquad (168)$$

Defining $t'' = t' + T$, Eq.(168) can be recast as

$$c_{n2} \cong \int_{-\infty}^{+\infty} dt' \langle n|z|i\rangle E_0 \sin(\omega t'') e^{-\frac{(t'')^2}{\tau^2}} e^{i\omega_{ni}(t''-T)}. \qquad (169)$$

$$\cong e^{-i\omega_{ni}T} \int_{-\infty}^{+\infty} dt' \langle n|z|i\rangle E_0 \sin(\omega t'') e^{-\frac{(t'')^2}{\tau^2}} e^{i\omega_{ni}t''}. \qquad (170)$$

$$\cong e^{-i\omega_{ni}T}\ c_{n1}. \qquad (171)$$

According to the linearity of the first order perturbation theory, the transition probability induced by the double weak pulse is

$$|c_n|^2 = |c_{n1} + c_{n2}|^2 \qquad (172)$$

$$= \left|c_{n1} + e^{-i\omega_{ni}T}\ c_{n1}\right|^2 \qquad (173)$$

$$= 4|c_{n1}|^2 \cos^2(\omega_{ni}T/2) \qquad (174)$$

The transition probability in Eq. (174) oscillates with the time delay between the two pulses and the frequency of oscillation is equal to the transition frequency between the initial and the final states. Therefore, we can obtain the spectrum of corresponding transition frequencies by Fourier transforming the transition probabilities with respect to the time delay. This is so called the Ramsey fringes. If it is possible to apply this in the neutral fragmentation experiment by using a double intense pulse, excitation probabilities show oscillative behavior in the time delay, which attributes to the oscillative behavior in the fluorescence signals as well. Thus if we Fourier transform a fluorescence signal, the peak position(s) tell us the transition frequencies from the ground state to the excited states in the parent molecule. In other words, if a fluorescing state are populated through more than one excited states in the parent molecule, the fluorescence signal should contain peaks at corresponding positions as finger prints. The Ramsey fringe however, is formulated using the first order perturbation theory, while we are interested in a highly nonlinear excitation process. Therefore we have to

confirm if it is applicable to the present problem. Certainly Ramsey fringe is not a general phenomenon. For example, Eq.(174) cannot be satisfied when $|c_{n1}|^2 > 0.25$, because its left hand side exceeds unity when $\cos^2(\omega_{ni}T/2) = 1$. This is one of the explanation why it is not applicable for intense fields. The basic idea behind the Ramsey fringe is the interference between two transition amplitudes independently created by respective pulses. As is discussed above, the key mechanism in the present nonlinear excitation process is nonadiabatic transitions between adiabatic Floquet states. As we see in Fig. 3-3(a), the nonadiabatic transition from the adiabatic Floquet state associated with the ground eigenstate is very weak. Therefore we can assume that the final transition probability after irradiating a double pulse is the consequence of the interference between the two transition amplitudes nonadiabatically created by the double pulse. This is why we expect that we can utilize the Ramsey fringe for the study of the excitation dynamics we are concerned in this thesis.

In order to confirm this idea, we calculated the excitation probabilities with an intense double Gaussian pulses as functions of the delay time. Here the wave length, the duration and the peak intensity are 800nm, 10fs , and 1.4×10^{14} W/cm^2, respectively. The polarization direction is along the z axis. After obtaining the transition probabilities as functions of the delay, we Fourier transformed it into the frequency domain. Fig. 3-5 shows the results. Here all the spectra are normalized so as that $\int_{-\infty}^{+\infty}|c_k\,(\omega)|^2\,d\omega = 1$.

In Fig. 3-5, the probabilities of the same principle quantum number show the same position of the peaks. The positions of the peaks of the eigenstates with the principle quantum numbers $n = 2,3,4,5$ are 0.3754, 0.4486, 0.4711, and 0.4799, respectively, which show almost perfect agreement with the transition frequencies from the ground state: 0.375, 0.445, 0.4687 and 0.48. The result shows that we can obtain the corresponding transition frequencies from the peak positions in the Fourier transformed probabilities. This clearly shows that Ramsey fringes is also practical in intense field case. We call this new experimental scheme

"Nonlinear Ramsey fringe". It should be noted here that our nonlinear Ramsey fringe is not a scheme that works with general nonlinear processes. It works only when the excitation mechanism is same as we discussed in this thesis. We believe, however, that the excitation mechanism discussed in this thesis is widely seen in atomic and molecular processes induced by intense laser field, so the applicability of our scheme is very broad.

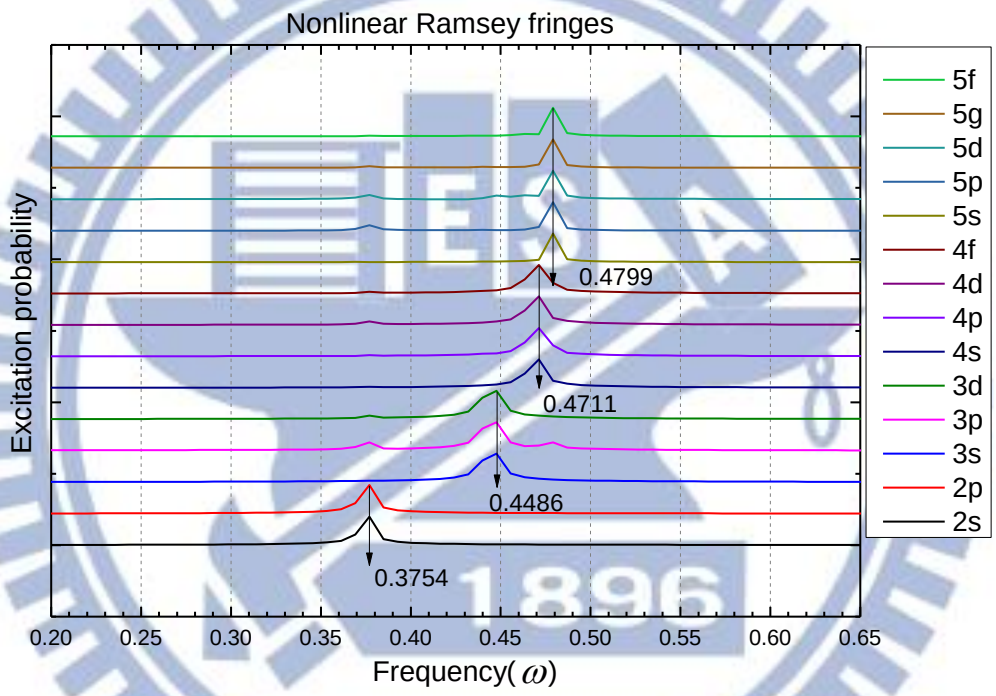

Figure 3-5 Fourier transforming the transition probability, which is induced by the double intense laser pulses, into frequency domain. Here, the pulse has intensity about 1.4×10^{14}W/cm^2. The laser pulse duration is about 10fs(FWHM), and the wavelength of the laser pulse is 800nm.

V. Summary

In this thesis, we discussed the highly nonlinear excitation process using the Fourier-Floquet analysis. Highly nonlinear excitation is one of the key mechanism in the neutral fragmentation, which has attracted a significant attention because of the possibilities in opening new applications of intense laser filed .

We first calculated the excitation probability of a hydrogen atom with the femto second intense laser fields as function of the intensity, and found interesting features: (1) the fluorescence signals have a power dependence on laser intensity, (2) the powers are very large ($n\hbar\omega$>ionization potential), and (3) Even (odd) angular momentum states have the power of 10(9).

In order to understand the excitation mechanism, we calculated the transition amplitude transformed into the frequency space, which we call the Fourier-Floquet spectra. Utilizing the idea of the Floquet theorem, the peaks in the spectra were analyzed. From the spectra. we found that the weave function is dominantly consists of the Floquet state that is adiabatically followed from the initial state, with a small portions of various nonadiabatically populated Floquet state, which attribute to the excitation process. Thus we analyzed them more carefully, and find that the nonadiabatic transitions dominantly occur between the Floquet states leading to the excitation to the same angular momentum parity states. Using this idea we succeeded to construct the detailed mechanism of highly nonlinear excitation. The key mechanism of this highly nonlinear excitation is the small nonadiabatic transition. This inspired us to propose a new experimental scheme for the direct measurement of the intermediate excited state. Here we used our finding that a simple interference pattern same as the Ramsey fringe is observed if we apply an intense double pulse.

Finally some future perspectives are mentioned here. In this thesis, we have obtained a

detailed knowledge on the Floquet states and the nonadiabatic transitions among them during the excitation process. We expect this knowledge combined with the strong field approximation will provide a new theory to predict the power dependence. Throughout this thesis we ignored the ionization processes, because we are interested in a qualitative understanding of the mechanism in the nonlinear excitation process. For the quantitative discussion, however, including continuum states are necessary.

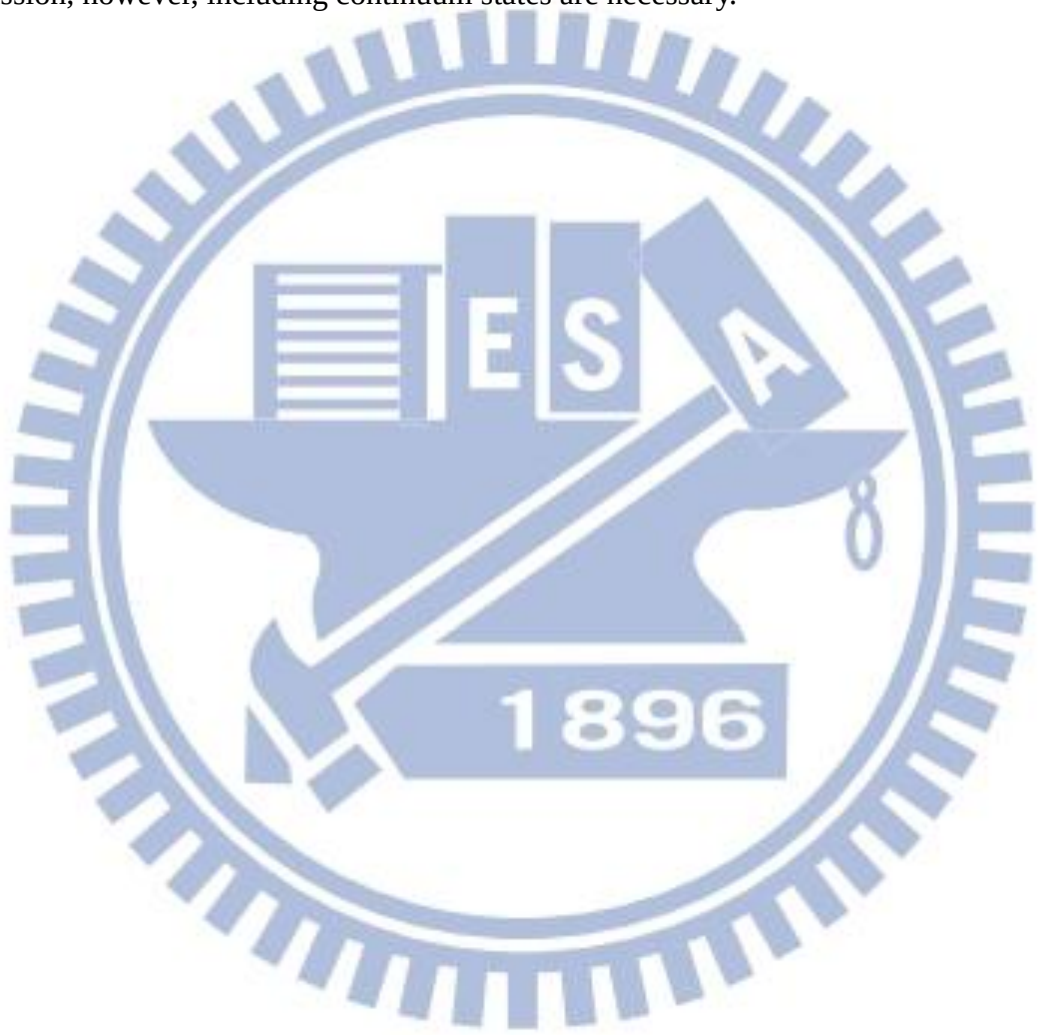

Reference

[1] Schawlow, A. L., and C. H. Townes, **(1958)**, *Phys. Rev.* 112,1940

[2] P. Agostini, F. Fabre, G. Mainfray, G. Petite, N.K. Rahman, *Phys. Rev. Lett.* 42, 1127**(1979)**

[3] U. Schwengelbeck, F.H.M. Faisal, *Phys. Rev.* A 50,632**(1994)**

[4] S. Augst, D. Strickland, D. D. Meyerhofer, S. L. Chin, and J. H. Eberly, *Phys. Rev. Lett.* 63, 2212 **(1989)**

[5] E. T. J. Nibbering, P. F. Curley, G. Grillon, B. S. Prade, M. A. Framco, F. Salin, and A. Mysyrowicz, *Opt. Lett.* 21, 62-64 **(1996)**

[6] A. Braun, G. Korn, X. Liu, D. Du, J. Squier, and G. Mourou. *Opt. Lett. 20*, 73-75 **(1995)**

[7] J. Kasparian, M. Rodriguez, G. Mejean, J. Yu, E. Salmon, H. Wille, R. Bourayou, S. Frey, Y. B. Andre, A. Mysyrowicz, R. Sauerbrey, J. P. Wolf, and L. Wöste, *Science* 301, 61 **(2003)**.

[8] L. Sudrie, A. Couairon, M. Franco, B. Lamouroux, B. Prade, S. Tzortzakis, and A. Mysyrowicz, *Phys.Rev. Lett.* 89, 186601 **(2002)**.

[9] M. Rodriguez, et al. Opt. Lett. 27, 9 **(2002)**.

[10] F. Kong, Q. Luo, H. Xu, M. Sharifi, D. Song, and S. L. Chin, J. Chem. Phys. 125, 133320 **(2006)**.

[11] A. Azarm, D. Song, K. Liu, S. Hosseini, Y. Teranishi, S. H. Lin, A. Xia, F. Kong and S. L. Chin, *J. Phys.* B: *At. Mol. Opt. Phys.* 44 **(2011)** 085601.

[12] Di Song, Ali Azarm, Yousef Kamali, Kai Liu, Andong Xia, Yoshiaki Teranishi, Sheng-Hsien Lin, Fanao Kong, and See Leang Chin, *J. Phys. Chem.* A **(2010)**, 114, 3087-3095.

[13] Kai Liu, Di Song, Ali Azarm, See-Leang Chin, Fan-ao Kon, *Chin. J. Chem. Phys*., Vol. 23, No. 3 **(2010)**.

[14] Y. Teranishi, M. Hayashi, F. Kong, S. L. Chin, S. D. Chao, H. Mineo and S. H. Lin, *Molecular Physics*, Vol. 106, Nos. 2-4, 333-339 **(2008)**

[15] T. S. Ho and S. I. Chu, *chem. phys. lett.* 141,315 **(1987)**

[16] S. I. Chu, *Adv. Chem. phys.* 73,379 **(1986)**